



**Politecnico
di Torino**

Master degree in Civil and Hydraulic Engineering

A.Y. 2025/2026

Master Degree Session 31/03/2026

**"Flow transients in water networks:
modeling and applications"**

Supervisor:

Prof. Riccardo Vesipa

Candidate:

Simone Toscano

Company tutors:

Ing. Luca Magni

Ing. Gianluca Colombo

Abstract

Water hammer in pressurized water hammer networks is one of the most critical aspects in the design and management of distribution systems. Sudden changes in flow rate, caused by the fast closure of a valve, the shutdown of a pump, or accidental events, generate pressure waves that propagate along the pipelines, producing overpressures and depressions that can be harmful to the structural integrity and reliability of the system. A correct analysis of transients is therefore essential not only to ensure the hydraulic operation of the network, but also to ensure adequate safety margins in exceptional operating conditions.

The present work analyzes the transient behavior of a real water network, with particular attention to the propagation, reflection and interference effects of pressure waves at nodes and geometric discontinuities. The study was carried out in collaboration with Studio Rosso Ingegneri Associati – SRIA (Torino), which provided the technical documentation relating to the case study and supported the development of the analysis.

The investigation has been developed through the application of the Method of Characteristics, implemented through a code written in a Python environment. The aim is to evaluate the spatio-temporal evolution of overpressures and verify the safety conditions of the system. The results show that in a complex network, the strongly interconnected structure and the presence of irregularities influence the effects of water hammer, making detailed dynamic analysis essential for the purpose of safe design and management.

Acknowledgements

The author would like to thank prof. Riccardo Vesipa for the guidance and support provided throughout the development of this thesis.

The author would also like to thank engineers Luca Magni and Gianluca Colombo of Studio Rosso Ingegneri Associati for providing the technical material and documentation used in this study. Their support and availability were essential for the development of the case study presented in work.

Table of contents

Introduction	1
CHAPTER 1 Method of Characteristics	3
1.1 Equations derivation	3
1.1.1 Continuity equation and momentum equation	4
1.1.2 Method of Characteristics	5
1.2 Energy explanation of water hammer	9
CHAPTER 2 Network model adjustments	11
2.1 Software presentation	11
2.2 Preliminary analysis with WNTR	11
2.2.1 Emitter coefficient addition	12
2.2.2 Valves replacement	15
2.2.3 Pipe length correction	16
2.2.4 Start/end nodes switch	17
2.5 Summary of preliminary operations	18
CHAPTER 3 Development of the Transient Model	20
3.1 Transients simulation with TSNet	20
3.1.1 Spatio-temporal discretization	20
3.1.2 Maneuver settings	21
3.1.3 Initial conditions and friction model	22
3.2 Starting of the simulation	24
3.3 Results database	25
CHAPTER 4 Application to Bari Sardo water network	28
4.1 Case study background	28
4.2 Water network configuration	29
4.2.1 Adduction pipeline	30
4.2.2 Distribution network	34
CHAPTER 5 Simulation of hydraulic transients	37
5.1 Network model pre-processing	37
5.2 Maneuvers	39
5.3 Summer scenarios	40
5.3.1 Results for summer scenarios	42
5.3.2 Detailed comparison of a closure maneuver	45

5.4 Autumn scenarios.....	53
5.4.1 Results for autumn scenarios	55
5.4.2 Detailed comparison of a opening maneuver.....	59
5.5 Safety checks and protection devices	66
5.6 Safe closure time evaluation.....	70
Conclusions	72
Appendix A	73
Appendix B	74
Appendix C	75
Appendix D	76
References	77

List of figures

Figure 1: characteristic lines schematization (source: TSNet official website)	8
Figure 2: spatio-temporal discretization (source: TSNet official website)	9
Figure 3: flowchart of the operations for emitter coefficients addition.....	13
Figure 4: flowchart of preliminary operations made by using WNTR	19
Figure 5: operation trend for a closure of 1 second (source: TSNet official website) ...	21
Figure 6: flowchart of the operations for the transient simulation analysis	25
Figure 7: scheme of the database structure for the results saving	26
Figure 8: map of Bari Sardo network representing both the adduction pipeline (red) and the distribution network (black)	29
Figure 9: new DN300 pipeline in purple and position of Connection "A"	31
Figure 10: enlargement on the position of bypass "A" and "B"	32
Figure 11: nodes supplied all year round (purple); nodes supplied by bypass "A" only during summer (orange); position of PRV "R2BS"	33
Figure 12: districts of Bari Sardo network	34
Figure 13: position of PRV "R3BS"	35
Figure 14: map of all the valves in the network of Bari Sardo	38
Figure 15: plot of the valve characteristic curve	39
Figure 16: gate valves status in summer configuration	40
Figure 17: enlargements of bypass "A"	41
Figure 18: enlargement of bypass "B"	41
Figure 19: histogram of maximum pressures for each maneuver in summer scenarios	42
Figure 20: histogram of minimum pressures for each maneuver in summer scenarios	43
Figure 21: focus on junction "P2"	44
Figure 22: location of the maneuver of valve "V5" shown with the red star	46
Figure 23: colormap of maximum pressure for each node in summer – Q = 20 l/s.....	47
Figure 24: colormap of maximum pressure for each node in summer – Q = 50 l/s.....	48
Figure 25: map of minimum pressure for each node in summer – Q = 20 l/s.....	49
Figure 26: map of minimum pressure for each node in summer – Q = 50 l/s.....	50
Figure 27: time series at the upstream node closing valve "V5"	51
Figure 28: time series at the downstream node closing valve "V5"	52
Figure 29: time series at node "J7" closing valve "V5"	53
Figure 30: gate valves status in autumn configuration.....	54
Figure 31: enlargements of bypass "A"	55
Figure 32: enlargements of bypass "B"	55
Figure 33: : histogram of maximum pressures for each maneuver in autumn scenarios	56
Figure 34: : histogram of minimum pressures for each maneuver in autumn scenarios	56
Figure 35: part of Gramsci district with the elevation in [m] for each node	57
Figure 36: time series at node "P5" closing valve "V47"	58
Figure 37: time series at the downstream node closing valve "V47"	59
Figure 38: location of the maneuver of valve "N1" shown with the red star.....	60
Figure 39: colormap of maximum pressure for each node in autumn – Q = 10 l/s; Cuccureddu alto district is highlighted in purple	61

Figure 40: colormap of maximum pressure for each node in autumn – $Q = 20$ l/s Cuccureddu alto district is highlighted in purple	62
Figure 41: time series at the upstream node opening valve "N1"	63
Figure 42: time series at the downstream node opening valve "N1"	64
Figure 43: time series at node "J7" opening valve "N1"	65
Figure 44: time series at node "4" opening valve "N1".....	66
Figure 45: collapsed pipe due to water hammer (source: Harper Haines website).....	68
Figure 46: scheme of air valve that lets air in due to pipe emptying (source: Vesipa R. Civil and industrial hydraulic systems – Lectures material, 2025)	69
Figure 47: scheme of air valve that lets air out due to pipe filling (source: Vesipa R. Civil and industrial hydraulic systems – Lectures material, 2025)	69
Figure 48: different closure time of valve "V5" after closing valves "V411" and "V49"	71

List of tables

Table 1: elements of the network.....	30
Table 2: valve closure curve	39
Table 3: summary for closures in summer scenario - $Q = 20$ l/s.....	73
Table 4: summary for openings in summer scenario - $Q = 20$ l/s.....	73
Table 5: summary for closures in summer scenario - $Q = 50$ l/s.....	74
Table 6:summary for openings in summer scenario - $Q = 50$ l/s	74
Table 7: summary for closures in autumn scenario - $Q = 10$ l/s.....	75
Table 8: summary for openings in autumn scenario - $Q = 10$ l/s	75
Table 9: summary for closures in autumn scenario - $Q = 20$ l/s.....	76
Table 10: summary for openings in autumn scenario - $Q = 20$ l/s	76

Introduction

The analysis of transient phenomena in pressurized hydraulic networks is a fundamental aspect for the design and verification of the safety condition of operation in water networks. The dynamic nature of the problem requires a modeling approach capable of capturing not only the magnitude of the overpressures, but also their evolution in time and space.

From a physical point of view, water hammer is a highly non-linear phenomenon, characterized by the propagation, reflection and transmission of waves in correspondence with geometric and hydraulic discontinuities. In simple systems, consisting of a single pipe, the behavior of the transient can be interpreted in a relatively intuitive way. However, when considering complex hydraulic networks, the problem becomes more articulated.

Contrary to what is expected, the high degree of interconnection of a network's structure does not automatically guarantee the rapid mitigation of water hammer. On the contrary, the presence of closed circuits, dead ends, variations in the characteristics of the pipelines and multiple reflections at the nodes can originate phenomena of constructive interference between the pressure waves, with the possible onset of locally high and unexpected pressure peaks. These effects can be particularly critical in specific areas of the network, even far from the point where the disruptive maneuver originates.

It follows that the transient behavior of a network does not depend exclusively on the operating conditions or properties of the individual pipelines, but is strongly influenced by the overall topological configuration of the system (R. Vesipa et al., 2025). The number of nodes, the degree of connection and the overall structure of the network have a decisive influence on the dynamics of overpressures and their spatial distribution.

In the light of these considerations, it is necessary to adopt calculation tools capable of accurately describing wave propagation phenomena. Among the available methodologies, the Method of Characteristics represents one of the most consolidated approaches for the solution of the equations of unsteady flow in pressure pipelines.

The present work is based on the application of the Characteristic Method for the analysis of hydraulic transients, implemented through a code developed in a Python environment. The analysis that will be described has been applied to a case study, in which the propagation of the effects of water hammer in a real network has been studied.

CHAPTER 1

Method of Characteristics

1.1 Equations derivation

The analysis of various flow phenomena in pressure pipelines requires models capable of describing the temporal evolution of the hydraulic quantities involved. In particular, the study of water hammer in complex hydraulic networks involves the solution of conservation equations of mass and momentum, written in the form of partial differential equations.

Among the different approaches proposed in the literature, the Method of Characteristics (MOC) represents one of the most widely used techniques for the analysis of hydraulic transients, as it allows the system of partial differential equations (PDE) to be reduced to a set of ordinary equations (ODE).

In the present work, the Method of Characteristics constitutes the theoretical foundation for the simulation of the dynamic behavior of pressure hydraulic networks subjected to water hammer. The analysis is focused on the phenomena generated by the opening or closing of a valve and it's conducted applying the MOC through a calculation code developed in a Python environment, capable of receiving a generic hydraulic network as input and returning the temporal evolution of pressures and velocity following a perturbation. Before proceeding with the analysis of the case study, it is therefore necessary to introduce the theoretical principles on which the method adopted is based.

In this chapter, the fundamental concepts of the Method of Characteristics applied to hydraulic transients are recalled, illustrating the basic hypotheses, the quantities involved and the equations used. This theoretical framework is essential to understand the choices made in subsequent analyses.

1.1.1 Continuity equation and momentum equation

The behavior of hydraulic transients in pressure pipelines is described by a system of equations that express the principles of conservation of mass and momentum applied to a compressible fluid flowing inside a deformable pipeline. The theoretical formulation presented in this chapter is based on the treatment provided in “*Applied Hydraulic Transients*” by M.H. Chaudhry (2014).

The continuity equation derives from the principle of conservation of mass and takes into account both the compressibility of the fluid and the elasticity of the pipe. In conditions of unsteady flow, a change in pressure leads to a change in the density of the fluid and a deformation of the section of the pipe, phenomena that are crucial in the propagation of the pressure waves associated with water hammer. The continuity equation (1) therefore relates the temporal variations of the hydraulic head with the spatial variations of the velocity along the conduit.

$$-\frac{\partial V}{\partial x} = \frac{g}{a^2} \frac{\partial H}{\partial t} \quad (1)$$

The equation of momentum (2), on the other hand, expresses the dynamic equilibrium between the forces acting on the fluid and the variation of its velocity in time and space. This equation allows to describe how changes in hydraulic head induce accelerations or decelerations of the flow, governing the dynamics of the transient.

$$\frac{\partial H}{\partial x} = -\frac{1}{g} \left[\frac{\partial V}{\partial t} + \frac{f|v|v}{2D} \right] \quad (2)$$

Both equations have been derived by neglecting the convective terms of the second order, that involve the terms in which the partial derivative of the velocity in space appears, since it is acceptable to consider that the variation of the velocity in space is negligible with respect to the velocity of propagation of the pressure wave.

Assuming a one-dimensional flow along the axis of the pipeline, the continuity equation and the momentum equation constitute a system of hyperbolic partial differential equations (3).

$$\begin{cases} -\frac{\partial V}{\partial x} = \frac{g}{a^2} \frac{\partial H}{\partial t} & \text{continuity equation} \\ \frac{\partial H}{\partial x} = -\frac{1}{g} \left[\frac{\partial V}{\partial t} + \frac{f|v|v}{2D} \right] & \text{momentum equation} \end{cases} \quad (3)$$

The term a represents the speed of propagation of the pressure wave and depends on both the properties of the fluid and the characteristics of the pipe. The term K represents the compressibility modulus of the pipe, E the elastic modulus, e the thickness of the pipe walls, D the diameter, and ρ the density of the fluid. The expression is shown below.

$$a = \sqrt{\frac{K}{\rho \left[1 + \frac{KD}{Ee} \right]}} \quad \text{pressure wave celerity} \quad (4)$$

1.1.2 Method of Characteristics

The equations that describe the hydraulic transients in pressure pipes are those given in the system of equations (3). These formulation, originally expressed in hyperbolic form, have been reformulated as a system of partial differential equations. Since it is not possible to derive an analytical solution in closed form, it is necessary to resort to numerical methods. As previously mentioned, among the different approaches available, the Method of Characteristics (MOC) has been adopted in this work.

Considering the system of equations (3), indicating L_1 as the first equation (5) and L_2 as the second (6), replacing the velocity V with the ratio between flow rate Q and pipe's cross section A , and introducing the term resistance R , defined as a function of the coefficient of friction f , diameter D and cross section A , are obtained:

$$L_1 = \frac{\partial Q}{\partial t} + gA \frac{\partial H}{\partial x} + RQ |Q| = 0 \quad (5)$$

$$L_2 = a^2 \frac{\partial Q}{\partial x} + gA \frac{\partial H}{\partial t} = 0 \quad (6)$$

Since both equations are zero, even a linear combination of them is zero. It's possible to write:

$$L = L_1 - \lambda L_2 = 0 \quad (7)$$

Replacing the equations L_1 and L_2 in the linear combination above (7), it becomes:

$$\left(\frac{\partial Q}{\partial t} + \lambda a^2 \frac{\partial Q}{\partial x}\right) + \lambda g A \left(\frac{\partial H}{\partial t} + \frac{1}{\lambda} \frac{\partial H}{\partial x}\right) + RQ|Q| = 0 \quad (8)$$

Since the flow rate Q and the hydraulic head H depend on both space x and time t , it is possible to introduce the concept of total derivative. By definition we have:

$$\frac{dQ}{dt} = \frac{\partial Q}{\partial t} + \frac{dx}{dt} \frac{\partial Q}{\partial x} \quad (9)$$

$$\frac{dH}{dt} = \frac{\partial H}{\partial t} + \frac{dx}{dt} \frac{\partial H}{\partial x} \quad (10)$$

Comparing these expressions with equation (8), the following conditions can be derived:

$$\begin{cases} \frac{dx}{dt} = \lambda a^2 \\ \frac{dx}{dt} = \frac{1}{\lambda} \end{cases} \quad (11)$$

Substituting these conditions in equation (8), we obtain the characteristic equation:

$$\frac{dQ}{dt} + \lambda g A \frac{dH}{dt} + RQ|Q| = 0 \quad (12)$$

Imposing the compatibility of the two conditions, we obtain:

$$\lambda a^2 = \frac{1}{\lambda} = \frac{dx}{dt} \Rightarrow \begin{cases} \frac{dx}{dt} = \pm a \\ \lambda = \pm \frac{1}{a} \end{cases} \quad (13)$$

In this way we obtain the two characteristic lines with slope $\pm 1/a$, along which the system reduces to ordinary differential equations.

From the previous relation (12) the following two equations can be written as:

$$\begin{cases} C +: \frac{dQ}{dt} + \frac{gA}{a} \frac{dH}{dt} + RQ \mid Q \mid = 0 & \text{along } \frac{dx}{dt} = +a \\ C -: \frac{dQ}{dt} - \frac{gA}{a} \frac{dH}{dt} + RQ \mid Q \mid = 0 & \text{along } \frac{dx}{dt} = -a \end{cases} \quad (14)$$

By moving along these lines in the spatio-temporal domain, it is possible to follow the evolution of the system and calculate the values of the hydraulic quantities in successive time instants starting from an instant t_0 in which the conditions are known.

From a physical point of view, this means that the initial conditions present at the point x_0 at the instant t_0 propagate both upstream and downstream along the two characteristic lines.

To determine the values of Q and H at a generic point P , located at $x = x_0$ at the instant $t = t_0 + \Delta t$, two known points A and B , upstream and downstream respectively, belonging to the positive and negative characteristics are used. By integrating equations (14) along the two lines, we obtain the following system.

$$\begin{cases} Q_P - Q_A + \frac{gA}{a} (H_P - H_A) + RQ_A \mid Q_A \mid \Delta t = 0 \\ Q_P - Q_B - \frac{gA}{a} (H_P - H_B) + RQ_B \mid Q_B \mid \Delta t = 0 \end{cases} \quad (15)$$

Schematically, the intersection of characteristic lines in the spatio-temporal domain can be represented as represented in figure 1.

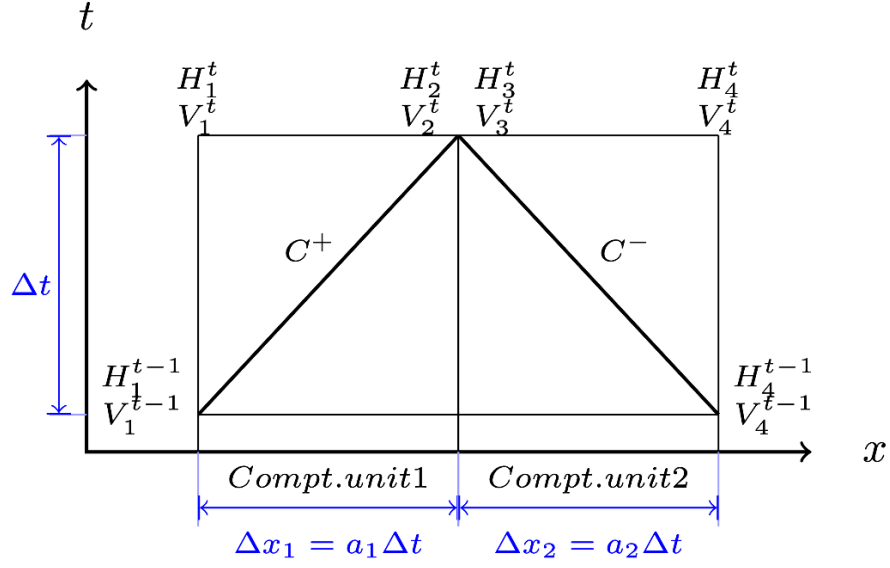


Figure 1: characteristic lines schematization (source: TSNet official website)

By introducing the terms C_P and C_N , which represent respectively the influence of the conditions propagated along the positive and negative characteristic, and defining $C_a = gA/a$, the system (15) can be rewritten in compact form as:

$$\begin{cases} Q_P = C_P - C_a H_P \\ Q_P = C_N + C_a H_P \end{cases} \quad (16)$$

from which we obtain:

$$\begin{cases} Q_P = \frac{1}{2}(C_P + C_N) \\ H_P = \frac{Q_P - C_N}{C_a} \end{cases} \quad (17)$$

To operationally apply the method, the pipes are discretized into a finite number of segments, dividing the spatio-temporal domain into intervals Δx and Δt , linked by the relation (18):

$$\Delta t = \frac{\Delta x}{a} \quad (18)$$

Through the discretization of the space–time domain, the characteristics from the adjacent nodes converge exactly at the central node at the subsequent time step. A schematization is provided in figure 2.

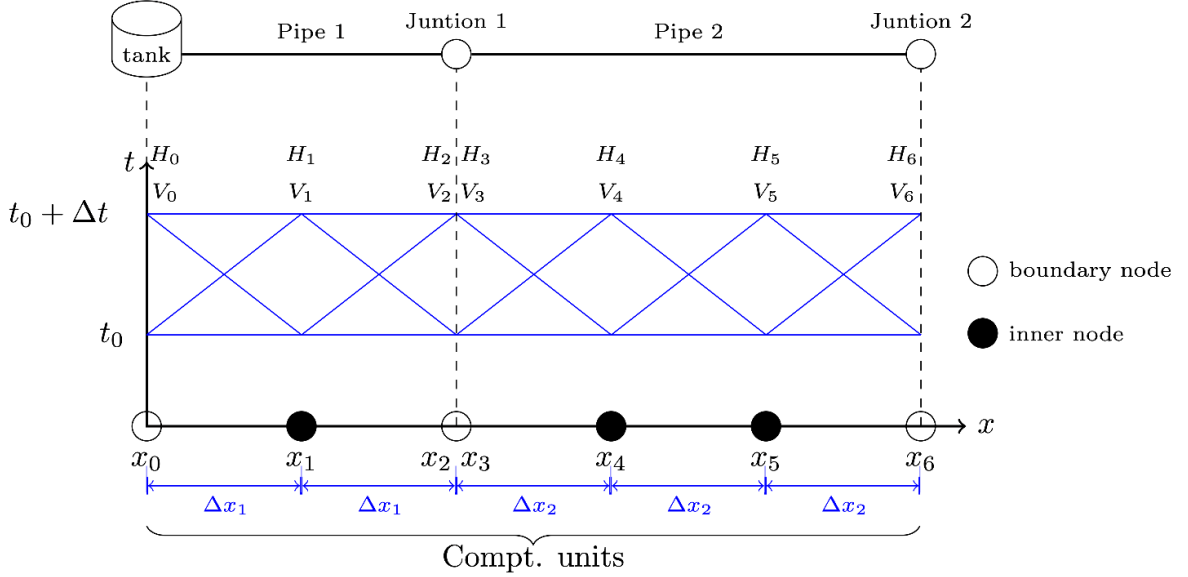


Figure 2: spatio-temporal discretization (source: TSNet official website)

For each node it is therefore possible to calculate the coefficients C_P and C_N , and determine the values of flow rate and hydraulic load at the new time instant. In practice, the calculation starts from the conditions of the steady state at the instant t_0 of time, applying boundary conditions dictated by the network configuration. In this way, the MOC allows to reconstruct the transient behavior of the network step by step over time, describing the propagation of pressure waves and the reflection and interaction phenomena that occur at the nodes and discontinuities of the system.

1.2 Energy explanation of water hammer

In a more intuitive way, the onset of the pressure wave can be explained in terms of energy balance. The water flowing within a pipe is characterized by a momentum that is a function of density and velocity. Therefore the energy of the fluid is the sum of the potential energy $U = f(H)$ and the kinetic energy $K = f(v)$. Assuming that the fluid is instantly blocked, the velocity becomes zero, as does the kinetic energy. This part of

energy is transformed into potential energy which manifests itself as a sudden increase of H. Since the elevation z remains constant, the increase in H manifests itself in the form of an increase in pressure. As in this case, for rapid manoeuvres the increase in hydraulic head can be obtained by means of the Joukowski relation. It is useful to remember that a maneuver is considered "fast" if it takes place in a time $T_o < T_c$ where T_c is the characteristic time of the conduct obtainable through the relationship $T_c = 2L/a$.

$$\Delta H = \frac{a\Delta v}{g} \quad \text{Joukowski's relation} \quad (19)$$

CHAPTER 2

Network model adjustments

2.1 Software presentation

This chapter describes the approach used to perform the simulation of hydraulic transients in complex hydraulic networks through codes written in the Python environment. The network on which the analysis is to be carried out was built on EPANET and subsequently translated into Python.

The main tool used is TSNNet (Transient Simulation in water Networks), which contains a series of libraries useful for the direct application of the Method of Characteristics. This tool makes it possible to effectively manage the maneuvers that cause water hammer and to simulate the consequent propagation of waves in the network.

In order to make the code more robust, flexible and compatible to hydraulic networks of any complexity, TSNNet has been supported by the WNTR (Water Network Tool for Resilience) library, used for the preliminary operations of network management and preparation. In particular, WNTR allows to resolve the network in steady conditions and to modify some properties of the elements that compose the network, just as it happens in EPANET.

It should be noted that TSNNet within the libraries makes use of WNTR to calculate the values of the hydraulic quantities involved to define the initial boundary conditions for the MOC, as a starting point at time t_0 . Despite this, it was still necessary to use WNTR before giving the input network to TSNNet in order to make the necessary changes to the network to optimize the computational performance of the simulation.

2.2 Preliminary analysis with WNTR

As anticipated in the previous paragraph, the WNTR tool has been used preliminarily on the water network in order to conduct a series of verifications useful for modifying some elements that compose it to make the code as robust as possible. Before starting with the

explanation of the operations carried out, it is useful to point out that WNTR offers two simulators to solve the steady state of a hydraulic network, namely "*Epanet.Simulator*" and "*WNTR. Simulator*" (Klise et al., 2017). In all operations where it is necessary to solve the water network in a steady state, "*Epanet.Simulator*" has always been used, with the exception of TSNNet which uses "*WNTR. Simulator*" in the calculation of hydraulic parameters for the initial boundary conditions.

Before giving as input the network to the Python code, according to the TSNNet user manual, it must be verified that the software limitation imposed on the topology of the network are respected. In short, demands cannot be assigned to the start and end nodes of pumps and valves, multi-branch junctions at these nodes are not supported, and pumps and valves must be connected in series by pipes. If one of these constraints is not met during the simulation, warnings are displayed showing a pressure discrepancy value. The larger the discrepancy, the poorer the quality of the results; in some cases, the result may not converge or may return incomplete time series.

2.2.1 Emitter coefficient addition

As first it's needed to export the file in which the network is created with the extension ".inp" through EPANET and load it into the script using the appropriate WNTR function. At this point, based on the conditions in which the simulation of hydraulic transients is to be carried out subsequently, it is necessary to specify the multiplier pt of the first time instant of the demand pattern assigned to the nodes, since it is the one with which TSNNet will calculate the starting data for the MOC at time t_0 .

It is possible to insert several demand multipliers if you want to simulate more scenarios in succession without having to manually modify them from EPANET. Based on the value given as input pt , the magnitude of that value is checked. If it is too large it can cause numerical instabilities in the simulations leading to incorrect results, so it is compared with a threshold pt_0 value set by default to 1, but editable if necessary. If the multiplier entered is greater than the threshold value, it would result in a flow coming out of the nodes Q_D greater than the flow rate that would occur with the multiplier pt_0 , called Q_0 .

$$Q_0 = demand * pt_0 * N_{junctions} \quad (20)$$

$$Q_D = demand * pt * N_{junctions} \quad (21)$$

To keep the flow rate Q_D leaving the nodes below the set threshold Q_0 , the difference in flow rate between and is applied as a leak of the pipes near the nodes, equal to Q_L , and not as a flow rate taken by the users.

$$Q_L = Q_D - Q_0 \quad (22)$$

Schematically the operations performed can be represented in the following way (figure 3), taking into account that the term "demand" represents the total base demand of the network.

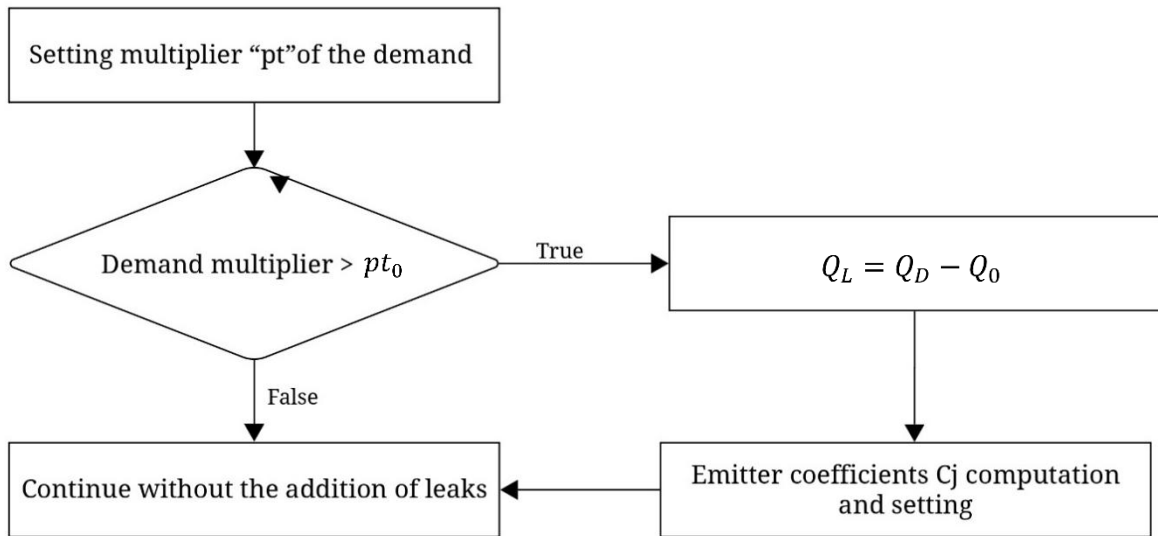


Figure 3: flowchart of the operations for emitter coefficients addition

Thus the demand pattern is forced to be equal to pt_0 and the flow rate subtracted by reducing the multiplier in each node is filled by adding it as a leak of pipes. This is not a simplification, but it is entirely acceptable since TSNet does not distinguish between the flow rate taken by users and the flow rate coming out of a leak. In both cases, the flow

rate is considered pressure-dependent and calculated using the exact same equation, that is the relationship that describes the flow from an orifice. Below is the formulation for a generic junction.

$$q_L = C_j * \sqrt{p_j} \quad \forall j - junction \quad (23)$$

At this point, it remains to calculate the emitter coefficient C_j at each node such as to cause an outgoing flow q_j necessary to fill the subtracted flow having reduced the demand multiplier. The coefficient C_j of can be obtained from the relation reported above for the orifice flow, but taking care to use the correct pressure value, which is the one that occurs when the multiplier of the pattern is equal to pt .

It is possible to obtain them by solving the aqueduct network in the steady state using the "*Epanet.Simulator*" function of WNTR. Having saved the steady state results for each element of the network, the inverse formula of the equation (22) can be carried out using the pressure of the node p_j and the flow rate q_L at the node , obtained by scaling the flow values referred to the entire network with respect to the number of nodes $N_{junctions}$, as shown below.

After defining the flow rate Q_L , the term q_L it is considered to be equally distributed among the nodes of the network and is computed as illustrated by the following relationships.

$$q_L = \frac{Q_L}{N_{junctions}} \quad (23)$$

$$C_j = \frac{q_L}{\sqrt{p_j}} \quad \forall j - junction \quad (24)$$

The values obtained in this way cannot be saved directly because WNTR does not support this function for emitter coefficients (unlike the other parameters), but they can be assigned by overwriting them directly in the ".inp" text file of the network automatically.

2.2.2 Valves replacement

The next step is the treatment of valves that apply a regulation in the network. From this point the operations carried out have not been performed by directly modifying the ".inp" text file, as for the emitter coefficients, but are done through the use of predefined WNTR commands to modify the parameters of interest and save them.

When placing a valve on EPANET it is possible to choose the type of valve and assign a status, which can be "open", "closed" or "none" (i.e. active). After performing preliminary tests on how TSNet works, it was observed that active valves, if not properly treated, can generate analytical discrepancies during the calculation of the MOC, affecting negatively the quality of the results.

For this reason, active valves with "none" status are replaced with a pipe of length L with a narrowing of diameter d . The value of d is appropriately calculated in such a way as to generate a concentrated head loss such as to produce the same effects as the valve does. This operation is permissible because the simulation of transients takes place in a time in the order of seconds or minutes, therefore the call flow rate from the network remains constant. In the event that it would be the case of interest, to adapt this change also to the steady state, it would be necessary to update the diameters of the narrowing from hour to hour according to the flow rate, but it is not of interest in this analysis. Below are the steps taken to calculate d for each pipe that replace a valve.

The formulation is derived from the Chezy's relation, where n is the Manning coefficient, R is the hydraulic radius and J is the piezometric gradient.

$$Q = \frac{1}{n} A R^{\frac{2}{3}} J^{\frac{1}{2}} \quad (25)$$

The terms R and J within the formula can be rewritten as follows:

$$R = \frac{A}{P} \quad (26) \quad J = \frac{\Delta H}{L} \quad (27)$$

R is defined as the ratio between the wetted area, which for pressure pipelines is equal to the cross section of the pipe, and the wetted perimeter of the conduit. The piezometric

gradient J , on the other hand, is given by the ratio between the hydraulic pressure drop H between the upstream and downstream nodes of the valve and the length of the pipe segment L that replaces the valve set at 20 meters. The choice of this length is not random and it will be discussed more in detail in the next paragraph. By inserting the expressions of R and J into the Chezy's relation, after a few mathematic steps, the following expression has been obtained:

$$d = \sqrt{\frac{4^{\frac{5}{3}} * n * Q}{\pi * J^2}} \quad (28)$$

After calculating the diameter of the pipe's narrowing d for each valve with active state, the modified network is saved in WNTR.

2.2.3 Pipe length correction

Proceeding with the sequence of operations, the next step is the modification of the length of the pipes that are too short. The greater the complexity of the network and the number of elements that compose it, the more important it is to carry out this modification since it greatly influences the time taken to perform the MOC simulation. If there are pipes in the network that are less than 10 meters long, the calculation time, after the start of TSNet, can extend by several hours and, in the case of very large networks, even for days. Of course, it is not practical to run a simulation of this duration, but it is fundamental to act on the right parameters to shorten the simulation time, in order to avoid to affect negatively the results by bringing a too high uncertainty. For example, increasing the simulation time step above the maximum threshold is not recommended, as it would contradict the Courant's criterion and the methodology of spatial discretization of the pipes adopted in TSNet. This aspect will be discussed in more detail in the chapter 3.

Then the analysis proceeds with a simple check of the length of the pipes L with respect to a threshold L_0 considering one pipe at a time and modifying it when L is less than L_0 , replacing L with the value of the fixed threshold.

The contribution of this modification to the model inevitably causes a slight loss of hydraulic pressure more than the original lengths because overall there are more meters of pipe in the network. The effect on the single pipe is quantified with a pressure drop of a few centimeters, depending on the roughness and how many meters of pipe have been added to reach the threshold L_0 . Imagining a scenario in which hydraulic transients cause pressure peaks of tens of meters, the reduction of the starting load by a few centimeters is negligible and therefore acceptable.

As in the previous case, the change in lengths is also saved on the WNTR template.

2.2.4 Start/end nodes switch

The last change that is made to the network is the way in which the starting node and the end node of the valves are defined, which having a status set to “*open*” or “*closed*” haven’t been replaced by a pipe’s narrowing. This operation is not essential for the correct performance of the calculation, but it is useful to make the results at the ends of the valves more clear. Adding a valve to the model defines the extreme nodes as *start nodes* and *end nodes*. If the flow rate flows from the *start node* to the *end node*, the direction is positive, and vice versa.

When the time series of the nodes upstream and downstream of the valve are extracted at the end of the transient simulation, TSNet is not able to identify the upstream and downstream nodes based on the direction of the flow rate, but always returns the *start node* as the upstream node and the *end node* as the downstream. When the time series are extracted at the ends of the valve, it therefore happens that in some cases the two nodes to which they refer are inverted, making the interpretation of the results less clear.

It is therefore useful to reverse the ID of the junction between the *start node* and the *end node*. This operation can be performed both before launching the TSNet simulation and during data extraction at the end of the simulation. It was decided to use the first choice and to apply the modification through WNTR.

2.5 Summary of preliminary operations

At the end of the preliminary operations, the WNTR model containing all the changes made to the network is saved and exported in ".inp" format so that it can be given as input to TSNNet, but also to be able to import it on EPANET and verify that all the corrections have been applied correctly.

Given a starting network, by using a loop the entire sequence of operations can be automatically repeated for each desired scenario by setting different values of the demand multiplier pt in a proper vector at the beginning of the code. This allows multiple simulations to be appended and to be performed with TSNNet automatically.

To summarize all the steps carried out up to this point, the following flowchart (figure 4) shows the sequence from importing the network to saving the modified version of it.

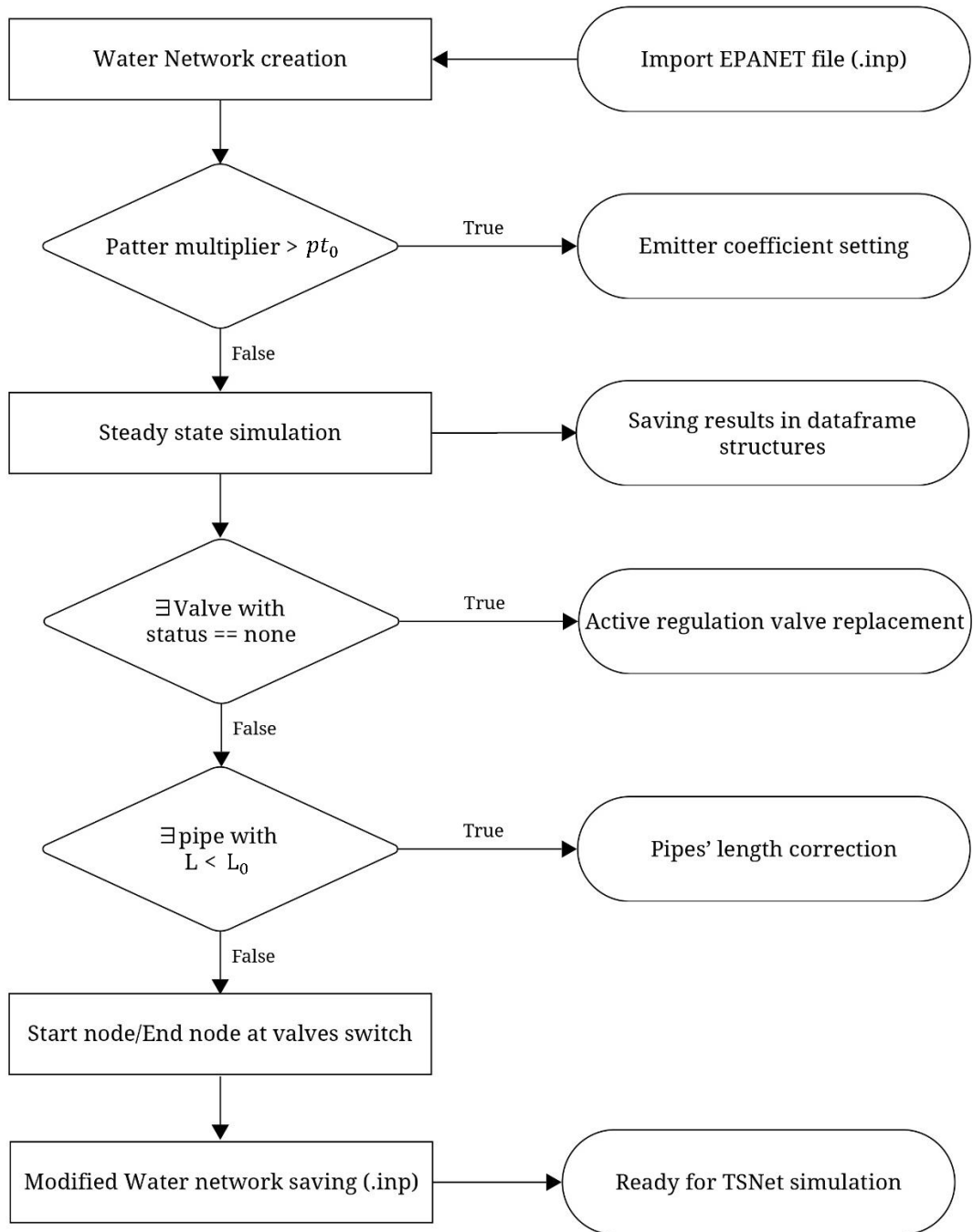


Figure 4: flowchart of preliminary operations made by using WNTR

CHAPTER 3

Development of the Transient Model

3.1 Transients simulation with TSNet

At this point in the analysis, the modified network is ready to be uploaded to TSNet and start the MOC (Lu Xing et al., 2020). Before doing this, it is necessary to set a series of parameters that govern the maneuver to be simulated, the simulation times and the friction calculation model. The following instruction have been written for the specific case of valve closure or opening, but the procedure still be the same for the other operations supported by TSNet.

3.1.1 Spatio-temporal discretization

Following the input order of the parameters, the first thing to define is the speed of propagation of the pressure wave. This value can be calculated using the formula (number) reported at the beginning of the previous chapter 2 or it can be used s value present in the literature. This value influences not only the physical phenomenon of wave propagation but also the simulation time since it is closely connected to the spatio-temporal discretization of the conduit and to the determination of the maximum usable time step Δt .

In TSNet, the value of Δt is computed by introducing the simplifying assumption that the velocity of the pressure wave is the same for all pipes and looking for the maximum possible value that respects two constraints. The first is the Courant criterion (number) given by the ratio between the length of a pipe segment and the speed of wave propagation, where L_i is the length of the pipe and is the number of segments N_i .

$$\Delta t \leq \min\left(\frac{L_i}{N_i a_i}\right) \quad i = 1, 2, \dots, np \quad (29)$$

The second constraint is that the time step is the same for all pipes. To satisfy this imposition, the term that varies is N_i the relation (number) can be rewritten as follows.

$$N_i = \frac{L_i}{\Delta t * a} \quad i = 1, 2, \dots, np \quad (30)$$

It is possible that the value of N is not an integer number, so it's necessary to round the value. So the value of Δt is unique for all pipes and it is allowed to enter one manually that is less or equal to the one calculated by TSNet, remembering that as the time step decreases and the time needed to run the simulation increases.

After this step, the duration of the simulation t_f must be chosen, which also includes the time needed to carry out the maneuver that gives rise to the water hammer.

3.1.2 Maneuver settings

In the next step, it is necessary to specify the parameters that govern the maneuver or event on which the transient calculation is to be carried out. TSNet supports several options, such as closing or opening a valve, pipe burst, pump shut off or turn on, and demand pulse. Since the case study examined in the next chapter analyzes the maneuvers carried out with the valves, the parameters concerning this case are reported below.

Must be set the duration time of the maneuver t_c , the time in which the maneuver begins t_0 , the percentage of the final opening se , where 0 corresponds to the total closure, and m the closing constant. The closing constant regulates the closure of the valve and if it is set to 1 it applies a linear closure, if set to 2 the trend is parabolic, as shown in the figure 5.

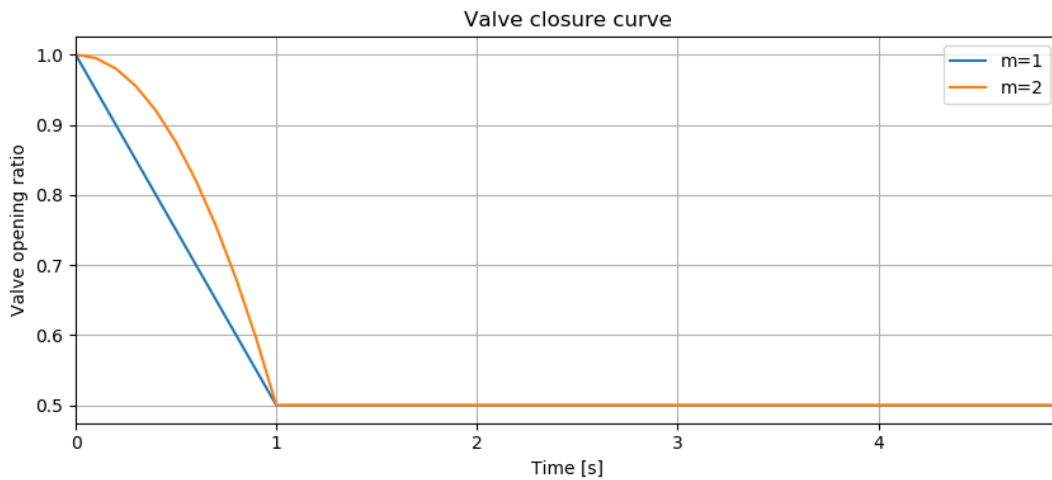


Figure 5: operation trend for a closure of 1 second (source: TSNet official website)

It is important to note that this feature is not always effective, in fact it may turn out that although the closure time is large the linear trend actually applies a closure similar to a sudden closure, giving results as output that are coherent with the Joukowski's relation. The cause is that TSNet does not simulate the closure as a reduction of the valve cross section, gradually bringing it to zero, but applies a minor loss coefficient K increasing over time.

The solution that has been adopted is to impose the values of minor loss coefficient K to be applied during closure through a function contained in TSNet. To apply it, it is necessary to define an *operation curve* consisting of two columns; the first includes the series of valve closure percentages and the second contains the *valve coefficients* , obtained as the reciprocal of the values of. In the case study examined in chapter 5 this operation will be clarified in more detail.

3.1.3 Initial conditions and friction model

The last settings to be specified before running the simulation are aimed at defining the steady state of the network, that is the starting point of the MOC, and the method by which TSNet manages friction. TSNet solves the network in steady state condition using WNTR and specifying if the computation has to be conducted in demand driven analysis (DDA) or pressure driven analysis (PDA). In DDA, the demand is always equal to the imposed one at junctions allowing the presence of negative pressure. In PDA, on the other hand, the pressure cannot drop below zero and in case of a too high demand, the flow rate it is reduced in order to keep a positive pressure.

If the steady-state calculation of the network is carried out using DDA, it is important that no negative pressures appear at the junctions; otherwise TSNet, which uses those values for the initial state conditions, generates incorrect results, obtaining a time series that diverges from the initial state.

The last step concerns the method used to compute the distributed head loss that occur along the pipelines. TSNet uses the Darcy–Weisbach equation for the calculation of pressure drops, regardless of the friction method specified in the EPANET ".inp" file.

Before starting the simulation, it is necessary to choose the method by which TSNet calculates the friction in the tubes between steady, quasi-steady and unsteady.

In the steady model, the pressure drops depend exclusively on the instantaneous velocity of the flow, similarly to what happens in a steady state; effects related to fluid acceleration are not considered. The coefficient of friction f is determined from the initial conditions of steady state, using the head loss h_{f0} per unit length and the initial velocity V_0 , where D is the diameter of the pipe and g is the gravity acceleration.

$$f = \frac{h_{f0} 2gD}{V_0^2} \quad (31)$$

During the transient simulation, the head loss per unit length is calculated just as a function of velocity and it's calculated as:

$$h_f = \frac{fV^2}{2gD} \quad (32)$$

In the present work for the case study in question, only the steady model has been adopted because, given the complexity of the network, this model being the simplest does not further slow down the time needed to carry out the simulation.

In addition to the steady model, TSNet allows you to adopt more advanced models, such as the quasi-steady and unsteady model. In the quasi-steady model, the formulation remains the Darcy–Weisbach formulation, but the coefficient of friction f is dynamically updated as a function of the Reynolds number for each time instant. The unit head loss therefore always depends on speed, but with parameters updated over time.

In the unsteady model, on the other hand, an non-steady contribution linked to the acceleration of the flow is added to the stationary component: $h_{fs} h_{fu}$

$$h_f = h_{fs} + h_{fu} \quad (33)$$

The non-steady component is calculated using Brunone's model:

$$h_{fu} = \frac{k_u}{2g} \left(\frac{\partial V}{\partial t} + a \operatorname{sign}(V) \left| \frac{\partial V}{\partial x} \right| \right) \quad (34)$$

Where the term $\frac{\partial V}{\partial t}$ represents the local acceleration, $\frac{\partial V}{\partial x}$ is the convective acceleration, a is the celerity of the wave and k_u is the Brunone coefficient, expressed as:

$$k_u = \frac{C^*}{2} \quad (35)$$

with:

$$C^* = \begin{cases} \frac{0.00476}{Re} & \text{moto laminare } (Re \leq 2000) \\ \frac{7.41}{Re^{\log(14.3/Re^{0.05})}} & \text{moto turbolento } (Re > 2000) \end{cases} \quad (36)$$

3.2 Starting of the simulation

At the start of the simulation, a selection of all the valves installed in the network is automatically done. Excluding valves with active control which, as explained above, have been replaced with pipes with a narrowing, the IDs of the open and closed valves are identified and saved in appropriate lists. Through the use of a loop, the simulation is automatically repeated for each valve by assigning a closing operation if the starting valve is open or an opening operation if the starting valve is closed. Now the model is ready to start the simulation using the MOC.

It should be specified that the loop that automatically runs the simulation for each valve is within the one specified at the beginning of the code based on the various demand multipliers chosen. So if, for example, in a network there are 2 open valves, 2 closed valves and three flow rate scenarios are set, entering three different *pt values*, a total of 12 simulations will be carried out.

The results of each simulation are automatically saved at the end in special data structures, from which it is possible to extract them and proceed with subsequent analyses. This will be discussed in the next paragraph.

To clearly summarize the operations carried out so far through TSNet, the following flowchart is reported (figure 6).

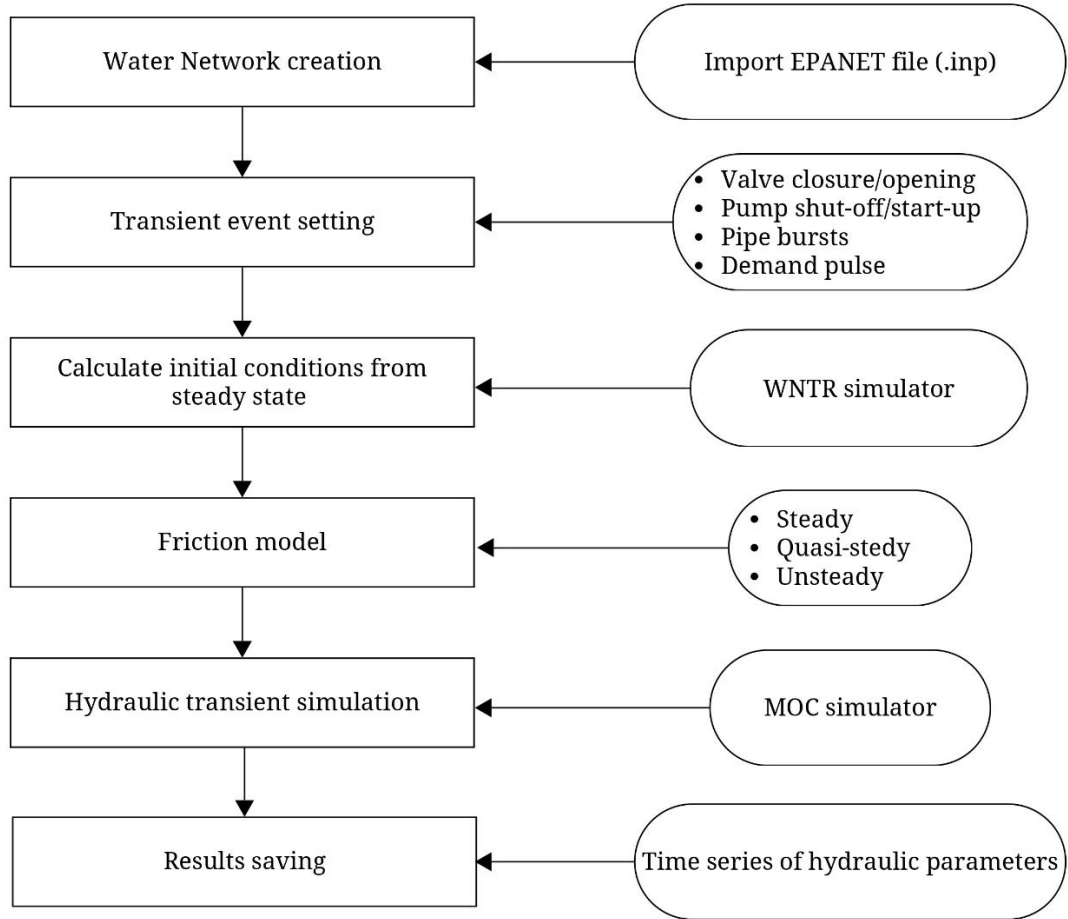


Figure 6: flowchart of the operations for the transient simulation analysis

3.3 Results database

At the end of each simulation, TSNet saves the results in ".obj" format from which it is possible to extract the time series of the parameters of interest. In the current work, the time series of the hydraulic load H at nodes and of the velocity V in the pipelines have been examined. For the purpose of assessing the criticality of the network in some nodes caused by water hammer, in this section checks are carried out on the values recorded and the data related to the elements involved are represented in a series of graphs. Since TSNet returns the hydraulic load data H , in order to obtain the pressure in meters of

water column, it is necessary to subtract the elevation of the node to which it refers from each value.

For the saving of the data and graphs produced, it is created automatically following a tree structure contained in the same folder where the file with the Python code is saved. The folder that is created is named "*Simulation patter_pt*", where *pt* takes the value of the demand multiplier used for the steady state calculation. To understand the structure contained inside, refer to the diagram below (figure 7).

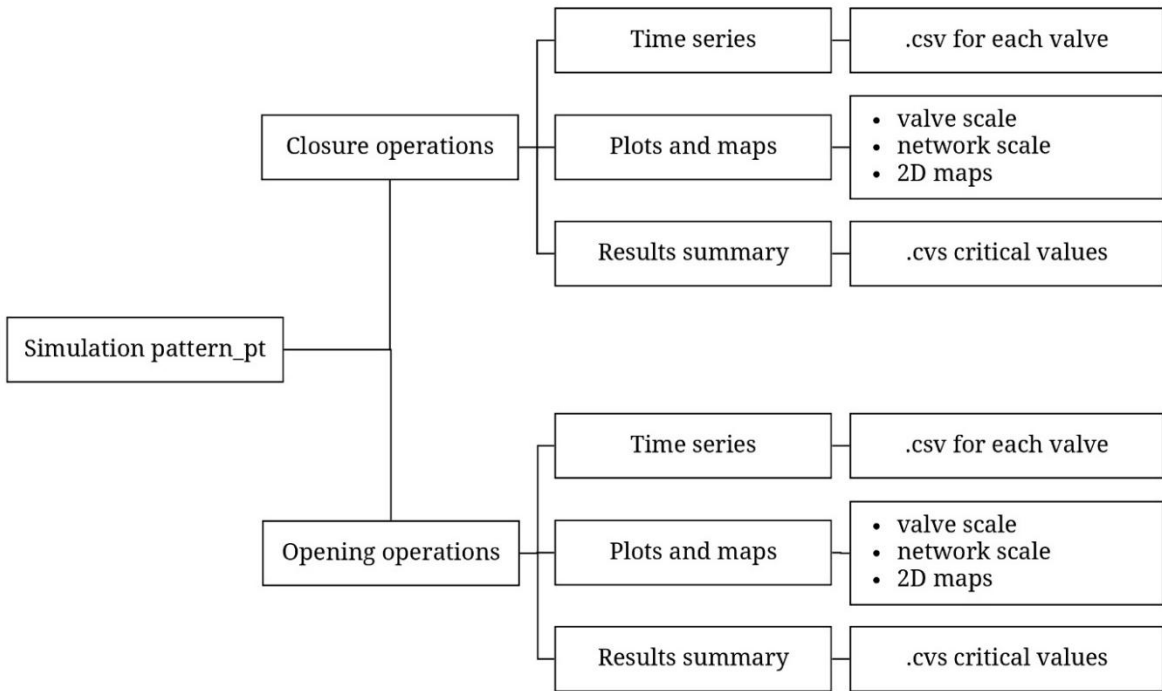


Figure 7: scheme of the database structure for the results saving

The ".csv" format files under the "Time series" folder contain the time series of the pressure at the nodes upstream and downstream of the valve, at the node where the maximum positive occurs, and at the node where the minimum value occurs.

The graphs show the time series of pressure and velocity in the nodes upstream and downstream of the valve, in the node where the positive maximum occurs and in the node where the negative maximum occurs. Three 2D maps of the network are then generated. The first represents the structure of the network with an indicator at the point where the maneuver took place; the second represents a colormap of the nodes based on

the evaluation of the maximum pressure in each node; the third instead considers the lowest pressure in each node by highlighting in red the nodes that reach a negative pressure.

Finally, a ".csv" file is produced containing a summary of all the maneuvers, reporting on each row a different valve and in the columns the maximum and minimum pressure value at the nodes upstream and downstream of the valve, the maximum in the network and the minimum.

In the next chapter the case study for which the procedure described was followed will be presented and the results of the analysis on hydraulic transients will be reported.

CHAPTER 4

Application to Bari Sardo water network

4.1 Case study background

The analysis of hydraulic transients according to the methodology described in this paper has been applied to the water network of the municipality of Bari Sardo, located in Sardegna, in the province of Nuoro. The network is managed by Abbanoa, which administers the water service of the entire region. The town is located 51 meters a.s.l. and it's about 3 km from the east coast. It has an average of 3900 residents and it's strongly influenced by the tourists in the summer months. In 2024, about 53264 stays were recorded in August (Istituto Nazionale di Statistica, ISTAT).

The entire network is supplied by gravity from the Cuccureddu tank, located in the western part of the town at an altitude of 83 m a.s.l., in turn fed by the Genna Masoni tank located at an altitude of 117 m a.s.l through the adduction pipeline that extends for about 12 km from south to north. Only in the summer months, to cope with the increase of the demand, a bypass is opened that puts the adduction in direct communication with the distribution network before the Cuccureddu tank. Despite the use of the bypass section, the large flux of tourists in the summer period causes peaks in demand in the order of 50 l/s that the network cannot provide. As a result, low pressure problems arise in areas where homes are only located at a higher altitude. Considering the critical issues encountered, a network improvement proposal was necessary, which was developed by the engineering firm Studio Rosso Ingegneri Associati. After detailed analysis of the network and the evaluation of possible solutions to improve its efficiency, the engineers proposed a new version of the network with a series of changes to existing elements and additional components. The analysis of hydraulic transients has been performed on the network project, including the changes proposed by the engineering company; The study was made possible by the technical documentation provided by the same. In the following paragraphs, the functioning of the network will be explained in more detail and then the results of the analysis conducted on water hammers will be discussed.

4.2 Water network configuration

The hydraulic network has a total of 414 nodes, of which 319 correspond to users, so they have an associated demand value. As mentioned in the previous paragraph, the network consists of two parts. The first consists of the adduction section that connects the Genna Masoni tank to the Cuccureddu tank and the second is the distribution network that connects the Cuccureddu tank to the users. Below there is the map of the entire network examined (figure 8).

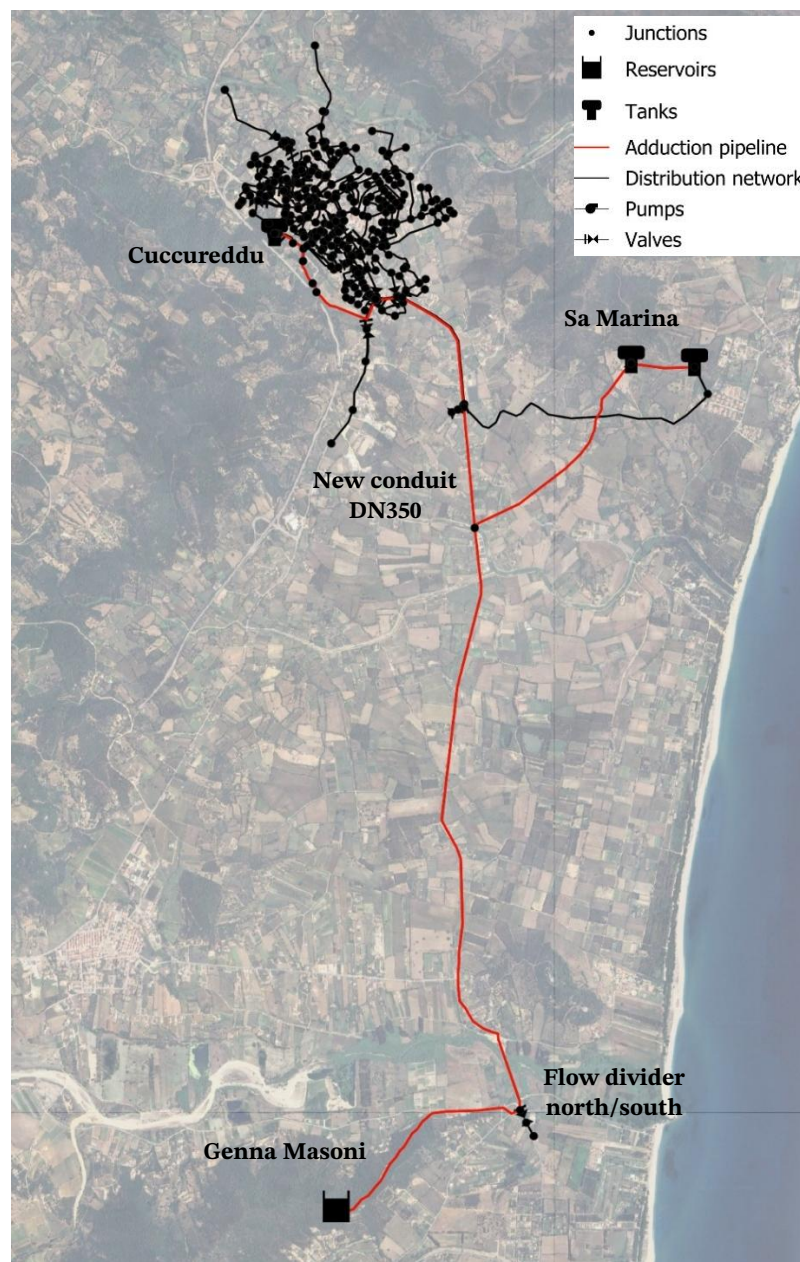


Figure 8: map of Bari Sardo network representing both the adduction pipeline (red) and the distribution network (black)

The Genna Masoni tank has a capacity of 150 m³ and is fed by three wells, each capable of delivering a flow rate of approximately 25 l/s, for a maximum of 75 l/s. Since there have never been any problems with water shortages from the wells, except during maintenance, Genna Masoni tank has been treated as a reservoir in the network model. As a result, it maintains a constant hydraulic head during the simulations.

Furthermore, the table 1 summarize the number of elements that form the network.

Nodes	Users	Pipes	Gate valve	PRVs	Pump	Tank	Check valve
414	319	461	24	5	1	3	1

Table 1: elements of the network

4.2.1 Adduction pipeline

The adduction pipeline extends for about 12 km and consists of cast iron pipelines with a diameter ranging from 200 to 350 mm. Following the direction of the flow, therefore from south to north, the first element encountered is the north/south divider, in which a portion of the flow coming out of the Genna Masoni reservoir is diverted to other users located to the south. At that point, a demand of 5 l/s was added to the model to take into account the flow rate subtracted. Continuing towards Bari Sardo, there is a branch that deviates from the adduction and feeds the Sa Marina reservoir. In the project scenario, thanks to the installation of a new pipeline with a diameter of 350 mm and 820 m long, the flow can continue towards the built-up area. As it stands, since it is not present, the entire flow is diverted towards the Sa Marina reservoir and then reconnected to the adduction.

The construction of the new pipeline with a diameter of 300 mm , highlighted in purple in figure 9, has made it possible to significantly reduce pressure drops, reducing the length of the pipeline in that section from about 4 km to 820 m. It can be seen that in addition to the Sa Marina tank there is a second tank, but it is no longer in use.

Furthermore, observing the same figure, there is a branch identified as "Connection A" which considers the various withdrawals distributed along the adduction pipeline as a concentrated demand in a point, in order to consider in the simulations a demand of about

1.5 l/s. Since the pressure on the supply is in the order of 10 m, the pressure reducing valve (PRV) "R4BS" has been inserted.

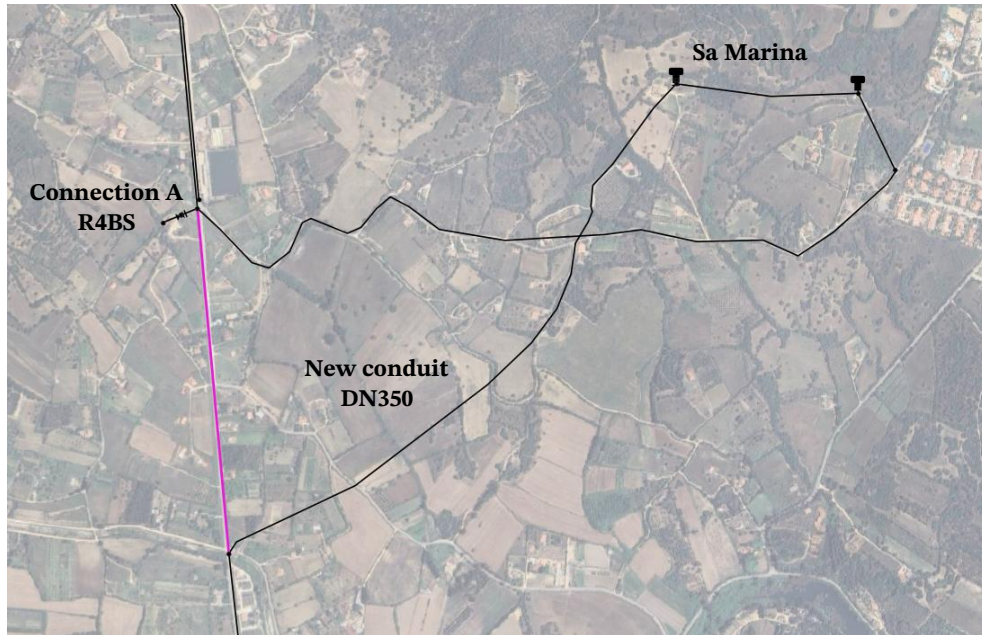


Figure 9: new DN300 pipeline in purple and position of Connection "A"

Continuing along the adduction line, the pipeline reaches the Cuccureddu reservoir, which can store up to 360 m^3 of water. Along this last section there are two branches that allow the direct connection of the distribution network to the adduction pipeline, bypassing the Cuccureddu tank, highlighted in blue in figure 10. In both branches there is a gate valve to be able to open and close the connections and a pressure reducing valve, respectively the "R1BS" and the "R5BS".

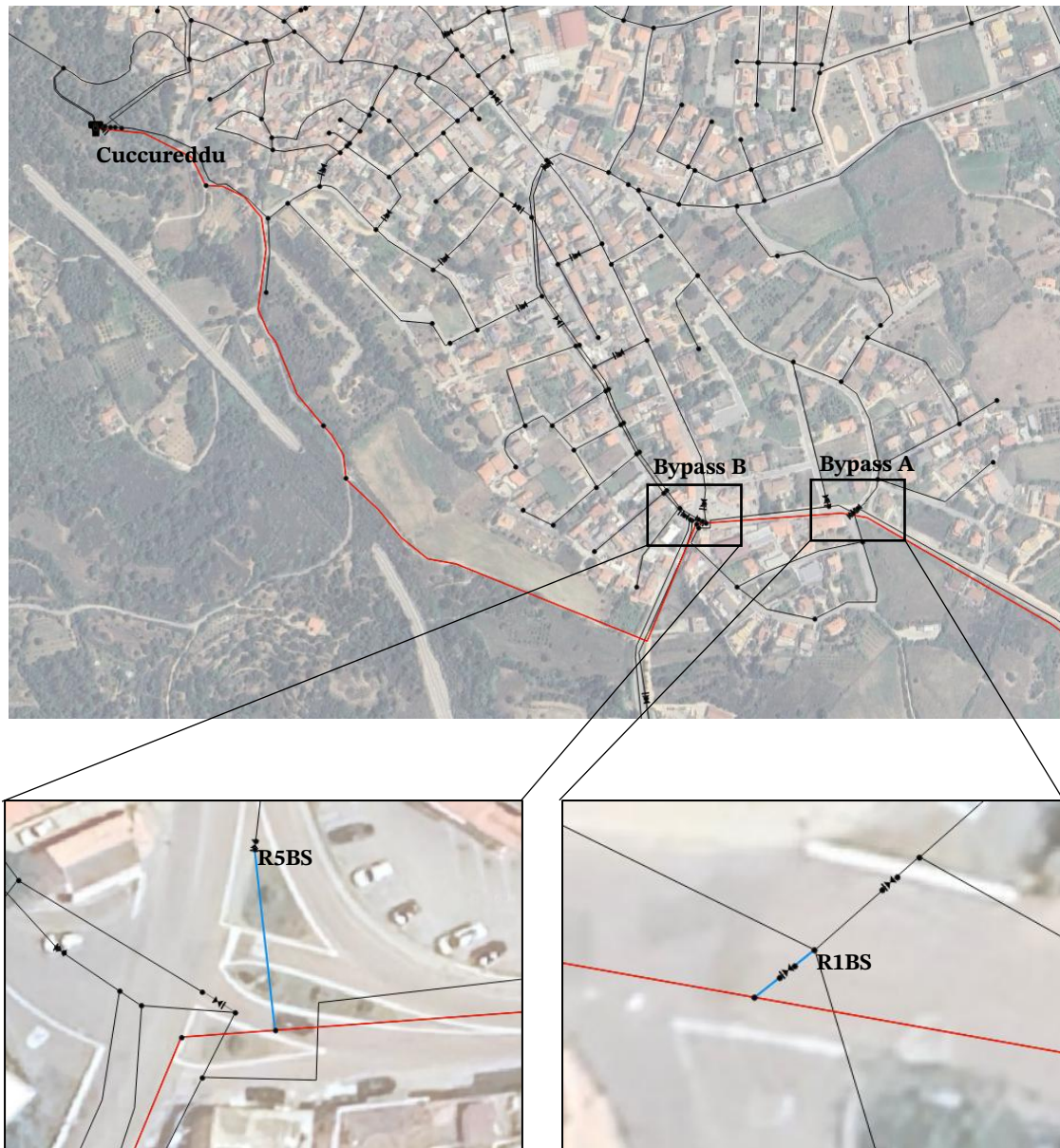


Figure 10: enlargement on the position of bypass "A" and "B"

Bypass "A" supplies the houses in the southern part, whose nodes have been highlighted in orange and purple in the figure 11, by means of pipes with a diameter between 125 and 80 mm. The nodes highlighted define the Gramsci district, which is the southernmost of the town. Bypass "A" remains open all year round, constantly supplying the nodes in purple. The nodes in orange, on the other hand, are supplied by bypass "A" only in the summer period; during the rest of the year they are gravity fed and the connection with bypass "A" is interrupted by closing the gate valve "N1" as will be shown at the start of

chapter 5. This section of bypass is already present in the actual configuration of the network, but the PRV valve and shutters have been added in order to have greater control and increase its resilience in case of maintenance. Note that the "R2BS" pressure reducing valve is installed on the branch that supplies some utilities in the southernmost part since the last node is at a lower altitude than the previous ones and it is necessary to reduce the pressure (figure 11).

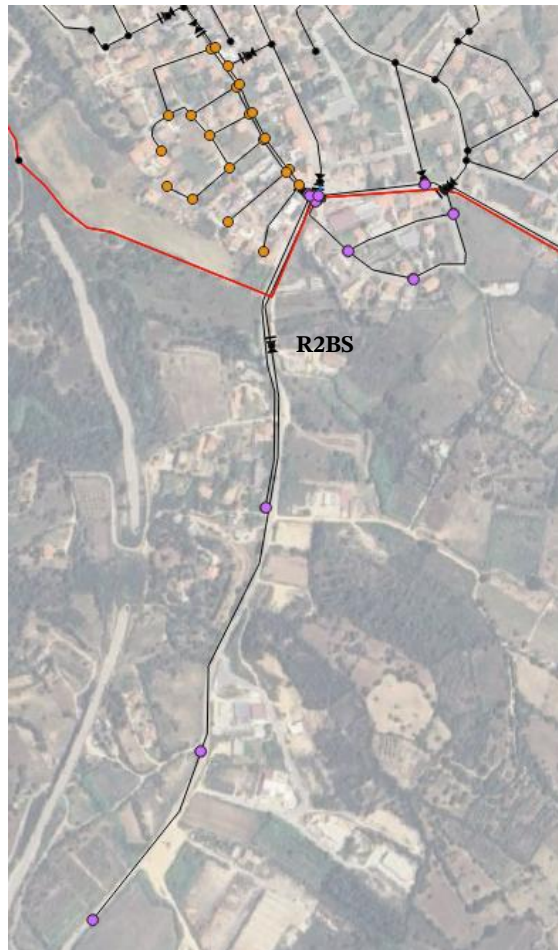


Figure 11: nodes supplied all year round (purple); nodes supplied by bypass "A" only during summer (orange); position of PRV "R2BS"

Bypass "B" is kept open only during the period of maximum water demand in the summer months and uses a pipe with a diameter of 200 mm. The pipeline of bypass "B" splits into progressively smaller branches moving towards the center of the network. When this bypass section is not in use, it is closed by means of the "V5" gate valve located upstream of the "R5BS" valve. Unlike the bypass "A", this connection is a project proposal to make the most of the 200 mm diameter pipe already present.

4.2.2 Distribution network

The distribution network, powered by gravity from the Cuccureddu reservoir located at 83 m a.s.l, serves 319 users located at various altitudes between 30 and 76 m a.s.l.. The houses are grouped into five districts, Cuccureddu alto, Cuccureddu basso, Gramsci, Mare and Tortoli. Applying a network districting is useful not only to monitor water consumption at various times of the year in each district, but serves as a tool to detect a leak more easily. The presence of gate valves that isolate the various districts is equally important because in the case of maintenance to a pipe, the district can still be temporarily supplied by another connection, avoiding the interruption of the water supply service. The figure 12 shows the districts of Bari Sardo.

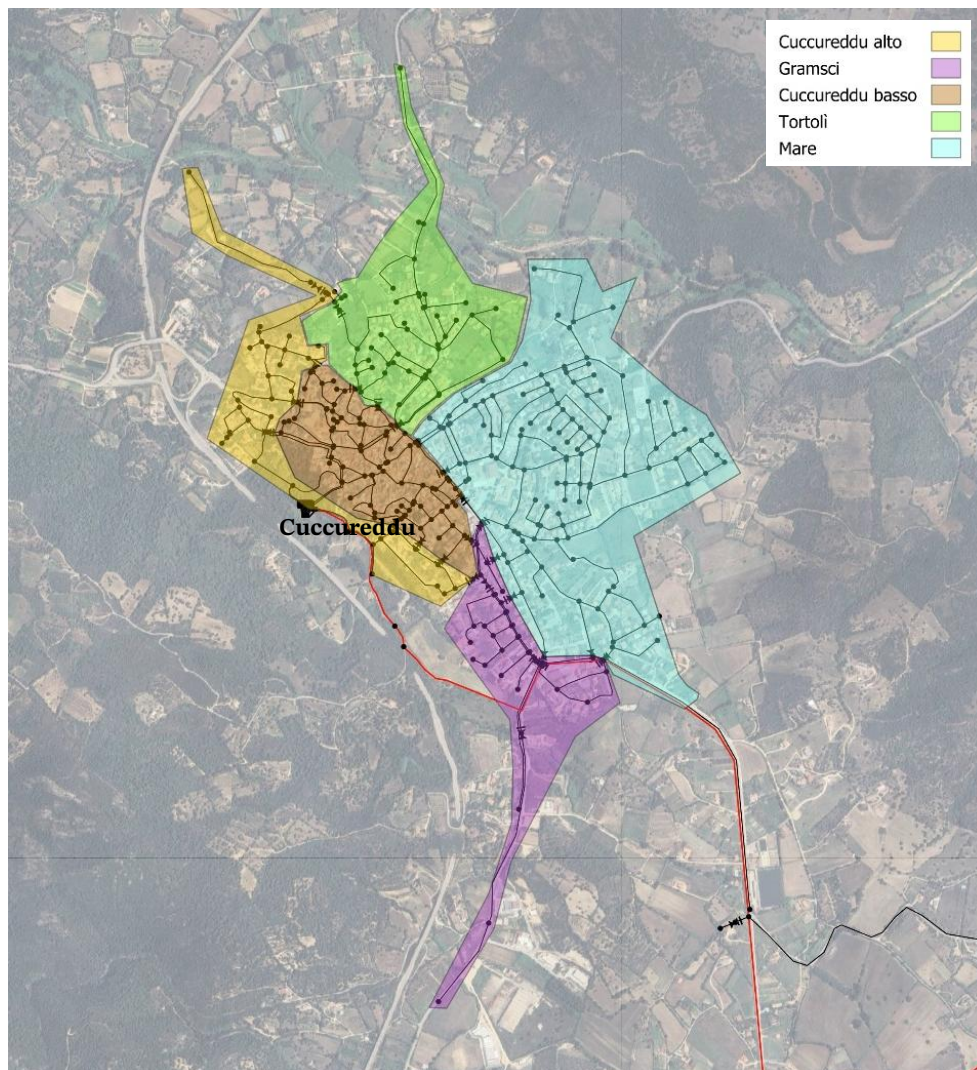


Figure 12: districts of Bari Sardo network

The districts of Cuccureddu basso, Mare and Tortoli are always gravity fed by the Cuccureddu reservoir since the houses are located at altitudes that do not exceed 50 m a.s.l.. In the upper Cuccureddu district, on the other hand, the houses were built at altitudes between 50 and 75 m a.s.l, so the pressure provided by the tank located at 83 m a.s.l is not always sufficient. To overcome this problem, the pipeline that feeds the district at high altitude is separated from the one that feeds the rest of the network and a pump has been added at the outlet of the tank capable of increasing pressures by about 20 m with a flow rate of 5 l/s. The district of Cuccureddu alto is separated from the rest of the network by a series of gate valves, which are kept closed.

Note that the junction in the northern part of the district is located at a lower altitude of about 30 m a.s.l. compared to the other nodes fed by the pump. It is therefore essential to install the "R3BS" pressure reducing valve. Figure 13 shows the detail of the PRV valve.



Figure 13: position of PRV "R3BS"

There are a total of 24 gate valves in the distribution network, some of which are periodically opened or closed depending on demand. During the summer months, demand fluctuates between about 20 – 50 l/s over 24 hours, while in autumn it is lower, such that it does not require the aid of bypass "B". Approximately 9 l/s of losses were estimated in the entire network, which were considered in the model together with user demand.

The other valves in the network are the five PRVs illustrated above and a check valve installed on the pipe leaving the Cuccureddu tank to prevent backflow during the night and the consequent flooding of the room.

In the project configuration examined, through the management implemented through the valves and shutters, the addition of the new pipes and the pump, the efficiency of the network is significantly improved. In the next chapter, a series of opening and closing maneuvers of the gate valves will be examined and through the application of the MOC the effect of water hammer in the network has been estimated.

CHAPTER 5

Simulation of hydraulic transients

5.1 Network model pre-processing

The first operation consists of performing the preliminary operations on the Bari Sardo aqueduct model in the design configuration using WNTR, following the procedure described in Chapter 2. The water network is composed of a total of 41.6 km of pipes, divided among 461 pipes. It is important to verify that the correction of the pipe lengths discussed in Section 2.2.4 does not cause excessive head losses. The minimum pipe length was set to 20 m; this value offers a suitable compromise between a clear reduction in the time required to run the transient simulation and, at the same time, the added distributed head losses are negligible.

In fact, the total length of the segments added to the various pipes having a length shorter than 20 m corresponds to 2.67% of the total kilometers of pipes in the network. Considering an average value of the distributed head loss per unit length expressed in m/km, the distributed hydraulic head loss amounts to approximately 33 m. Distributing this value among the pipes in the network, each pipe is associated with a value of 0.07 m, i.e., 7 cm. This value is negligible compared to the scale at which water hammer occurs; therefore, the correction of the pipe lengths is acceptable. The time required to run the simulation for all the valves in the network was reduced from approximately 30 hours to approximately 5 hours.

With regard to the setting of the emitter coefficients, the threshold of the demand multiplier pt_0 was set to 1.35, corresponding to 20 l/s demanded from the network. Only in the simulated scenarios in which the multiplier pt is greater than 1.35 are emitter coefficient values assigned, as explained in Section 2.2.2.

Before proceeding with the discussion of the executed maneuvers, the network layout showing the position of all the valves present in the design scenario is reported below (figure 14).

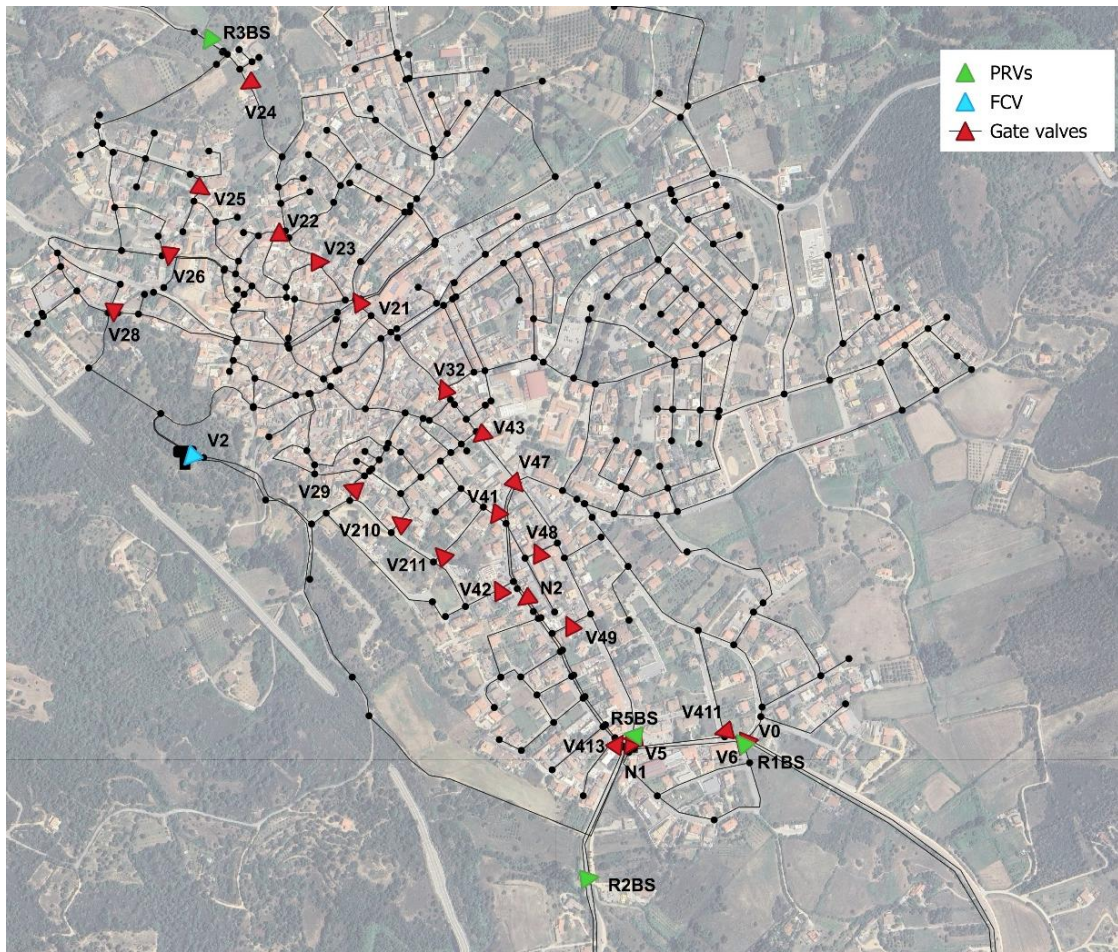


Figure 14: map of all the valves in the network of Bari Sardo

It should be noted that the valve “V2”, highlighted in blue, is not included in the design but was introduced in order to regulate the flow rate, and consequently the pressures, along the final section of the adduction main, both to limit the flow rate to a value closer to the real one and to prevent the simulation from diverging from the solution, as explained in Section 2.2.1. In the simulations, the valve “V2”, having a status corresponding to “none”, was treated in the same way as the PRVs, replacing it with a calibrated restriction according to the methodology described in Section 2.2.3.

5.2 Maneuvers

The hydraulic transient simulations were carried out on four different configurations of the Bari Sardo network, and for each gate valve an opening or closing maneuver was executed. All maneuvers were performed over a duration of 80 seconds and the valve closing or opening time t_c is equal to 10 seconds. Since the pipes are mainly made of cast iron and steel, the pressure wave propagation velocity a is assumed equal to 1200 m/s. A slow maneuver is intended to be simulated, but the default TSNet setting with $m = 1$ actually produces the same effect as an instantaneous closure. For this reason, as explained in Section 4.1.2, it is necessary to manually set the values of the ratio $1/K$ in order to produce the effects of a slower and linear closure. The values used for all simulations are reported in table 2.

% opening	1/K
100	1
90	0.1
80	0.01
70	2.0E-03
60	1.0E-03
50	5.0E-04
40	2.0E-04
30	1.0E-04
20	5.0E-05
10	2.0E-05
5	1.0E-05
0	0

Table 2: valve closure curve

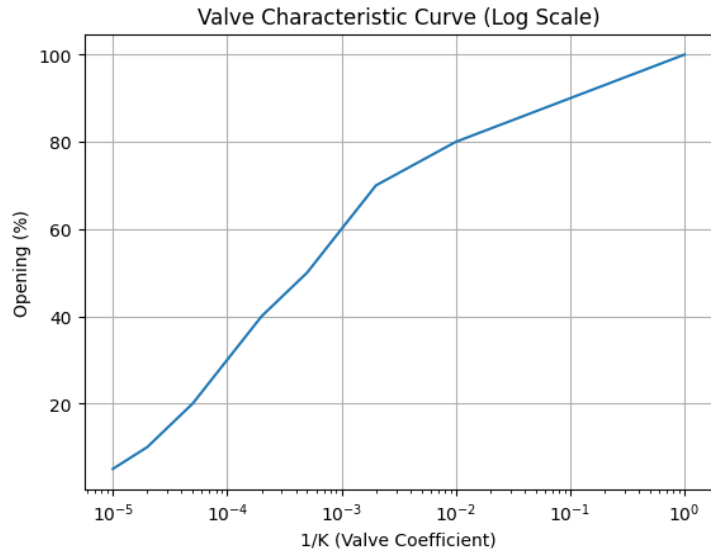


Figure 15: plot of the valve characteristic curve

The steady-state calculation, which defines the boundary conditions for the MOC, was carried out in DDA, while for the friction calculation the steady model has been selected. During the code validation phase, the same maneuver was simulated using the three friction models; however, no difference emerged in this case study when comparing the results, and moreover the time required to run the code approximately doubled when using the unsteady model.

5.3 Summer scenarios

The objective of the hydraulic transient analysis applied to the Bari Sardo water network is to quantify the intensity of the water hammer by performing the same opening and closing maneuvers of the gate valves under different network usage conditions. Four scenarios were simulated, two representing operating conditions during the summer months and two during the autumn months.

In the summer scenario, both bypasses “A” and “B” are open, the pump is active, and among all the gate valves, four are open: valve “V5” that act on bypass “B”, “V6” which act on bypass “A”, “V22”, and “N1”. In the map (figure 16), the configuration in the summer scenario is shown, highlighting the open and closed valves.

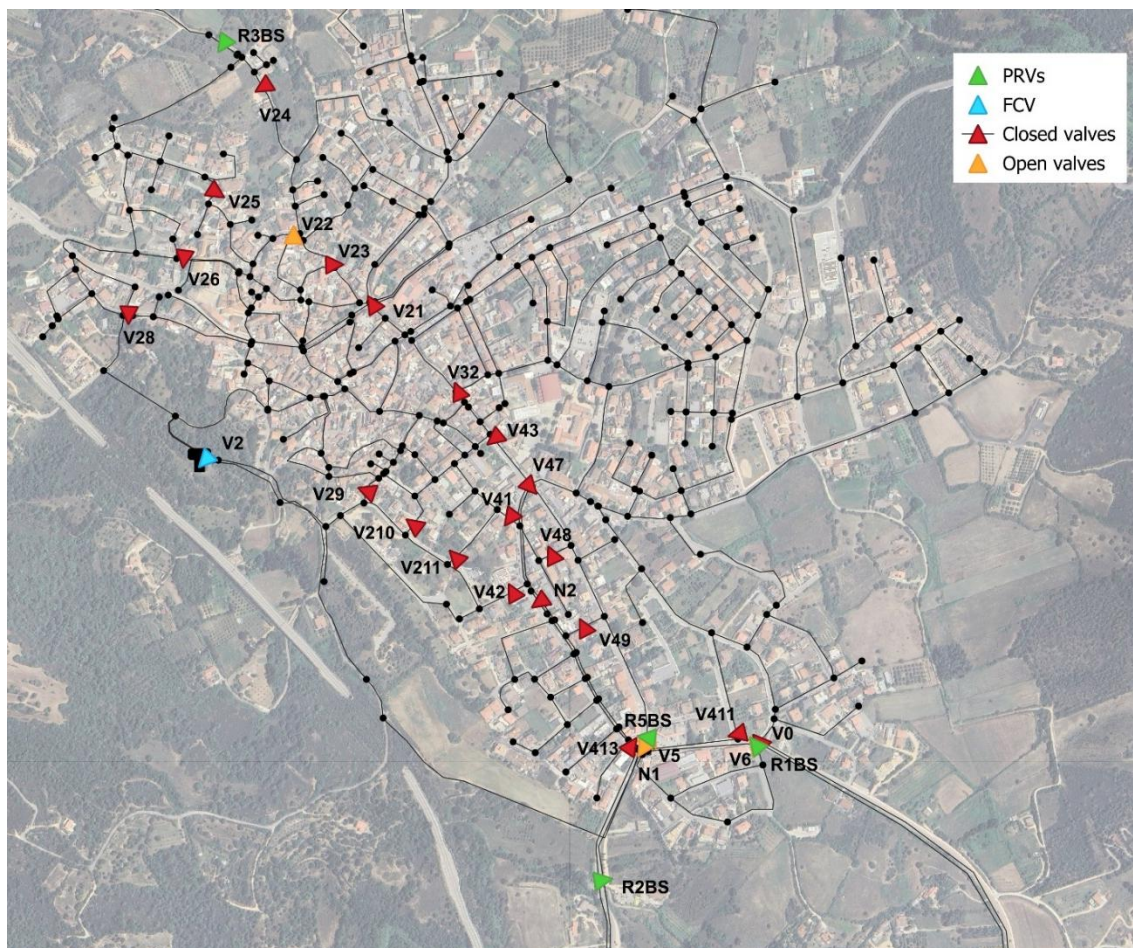


Figure 16: gate valves status in summer configuration

A local enlargement in the vicinity of bypasses “A” (figure 16) and “B” (figure 17) is also reported.

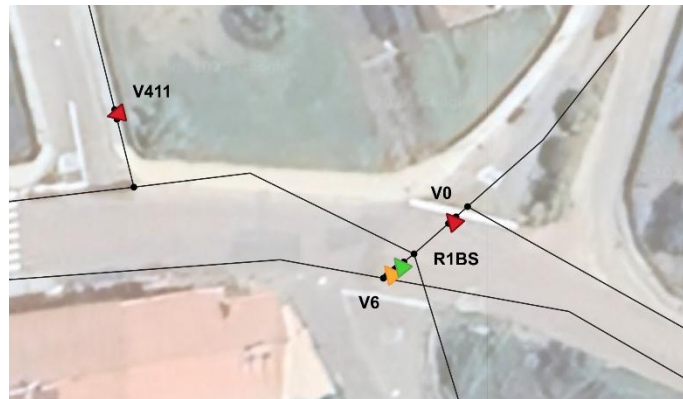


Figure 17: enlargements of bypass “A”

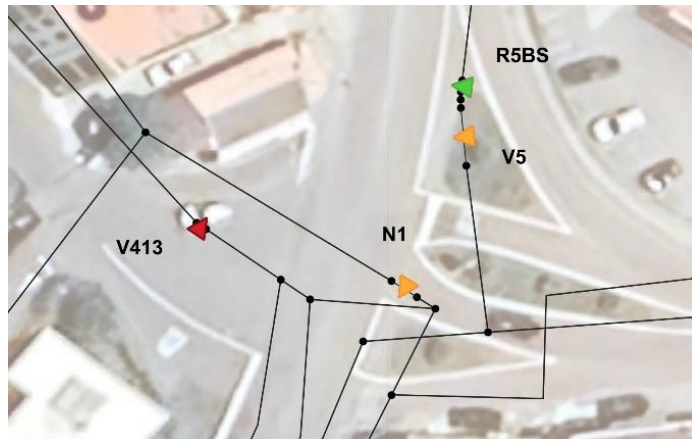


Figure 18: enlargement of bypass “B”

The effect of water hammer during the summer period was evaluated in the case in which it occurs during the day, imposing 45 l/s demanded from the network, and during the night, assuming 20 l/s demanded. Both demand values also account for aqueduct losses and, given the withdrawals along the aduction main, up to 54 l/s flow downstream of the Genna Masoni reservoir. With both bypasses open, only a small portion of the flow rate arriving from Genna Masoni continues toward the Cuccureddu tank. To reproduce conditions as close as possible to the real ones, by means of the FCV “V2” the inflow to the reservoir was limited to 8 l/s during the day and 14 l/s during the night.

5.3.1 Results for summer scenarios

The results obtained from the simulations in the two summer scenarios were collected and compared using histograms. The first graph (figure 19) shows the maximum pressure reached in the network following the closing maneuver (in blue) or the opening maneuver (in green) for each valve.

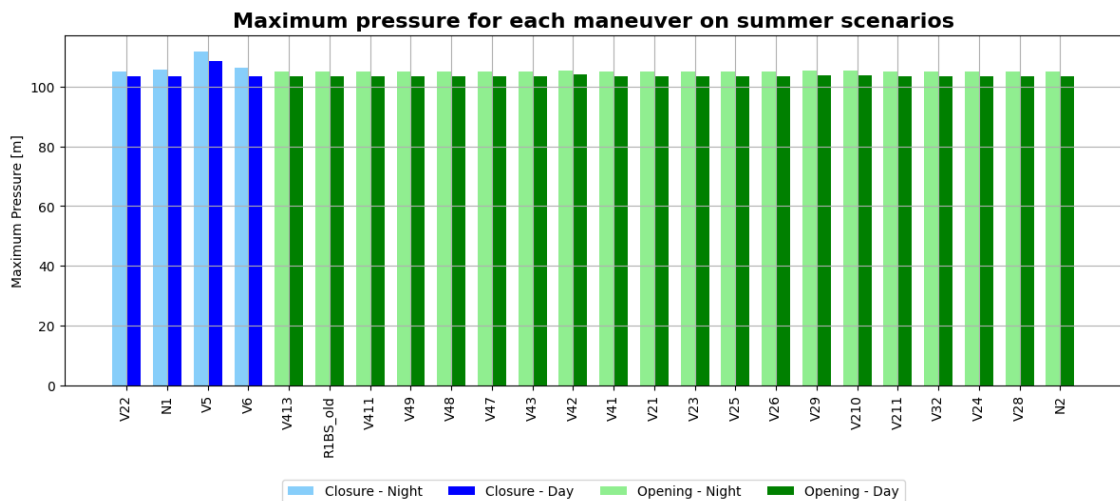


Figure 19: histogram of maximum pressures for each maneuver in summer scenarios

It can be observed that the maximum value reached is approximately the same, about 107 m, except for valve “V5”, which reaches 111 m. These values are reached for all maneuvers at node “J7”, which is located on the adduction line about 1.5 km from the Genna Masoni reservoir, close to the north–south divider.

The reason why the maximum pressure value is recorded at this node is that, through a slow valve closure performed in 10 seconds, the water hammer produces a pressure peak in the nodes of the distribution network that is always lower than the pressure in the adduction line. In fact, node “J7” is located at an elevation of 6.3 m a.s.l and the steady-state pressure is equal to 105 m. The nodes of the distribution network are instead located at higher elevations and the maximum pressure values recorded are always lower than 74 m. If the closure were faster, it is highly likely that in some nodes of the distribution network pressures higher than those in the adduction line could be dangerously reached. Despite the maximum pressures being very similar among the maneuvers, valve “V5”

appears to be slightly the most critical. This result is consistent with expectations, since the gate valve “V5” acts on bypass B, where a flow rate of about 15 l/s occurs, which is at least three times greater than the flow circulating in the other main supply branches equipped with gate valves.

Regarding negative pressures, the results for all maneuvers were reported in a histogram similar to that of the maximum pressures (figure 20). In addition, the initial pressure values of the nodes where the minimum pressure occurs were represented by the grey bars. These values correspond to those calculated in steady-state conditions just before the beginning of the maneuver.

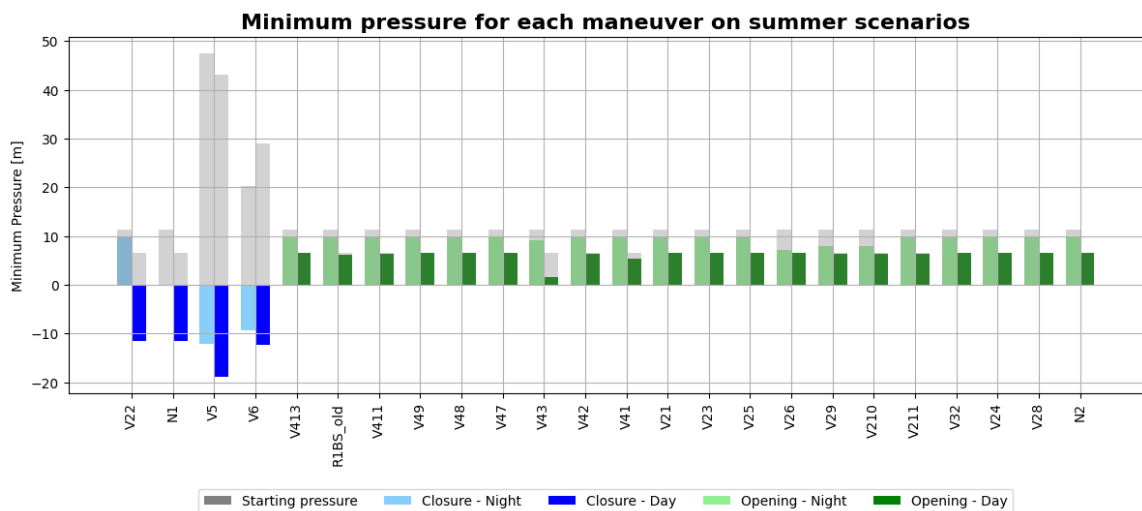


Figure 20: histogram of minimum pressures for each maneuver in summer scenarios

First of all, it can be observed that opening maneuvers are less dangerous than closures, since negative pressures are never reached. The most critical gate valve is “V43”, which reaches a minimum pressure of about 2 m in the daytime scenario. In this regard, it is good practice to consider a safety margin in order to avoid approaching zero too closely, with the risk of reaching negative pressures in case of slightly different initial conditions than those simulated. It should also be noted that all opening maneuvers reach the minimum pressure at the same node, identified as “P2”. This junction is located on the adduction line just before the Cuccureddu tank, as shown in figure 21.

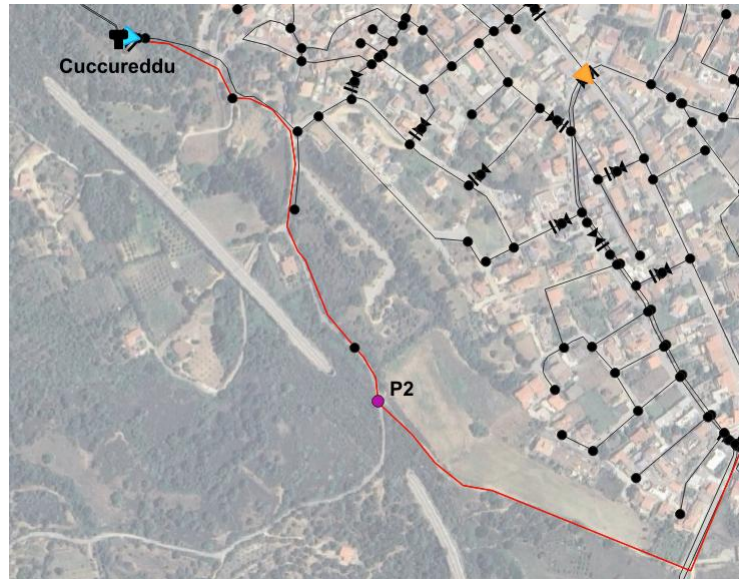


Figure 21: focus on junction "P2"

Node “P2” is located at an elevation of 93 m and is the highest node along the adduction pipeline. Even under steady-state conditions it is a critical junction because the pressure is low, since the pipe rises towards the Cuccureddu tank.

Observing the closing maneuvers, on the other hand, the greater criticality and danger of these maneuvers immediately becomes evident. In fact, not only do pressure values below 10 m occur, but especially for valves “V5” and “V6” the Δp between the initial pressure and the minimum pressure in the node, represented by the difference between the colored bars and the grey bars, is very high. Also with regard to negative pressures, valve “V5” appears to be the most critical for the integrity of the network. As described in Section 3.3, at the end of each simulation a summary table of the performed maneuvers is automatically generated, containing the key values for each of them.

The summary tables for the nighttime summer scenario ($Q = 20$ l/s) are reported in Appendix A, while those for the daytime scenario ($Q = 50$ l/s) are reported in Appendix B.

5.3.2 Detailed comparison of a closure maneuver

As an example, the time series of pressure and velocity for a single maneuver are reported and compared between the two scenarios. The maneuver considered is the closure of valve “V5”, since it is the most representative of the problem under investigation, as emerged from the previous discussion. Before commenting on the time series related to the maneuver, some maps useful to identify where the maneuver occurred and what effects were produced in the network are reported. In graph (figure 22) the network layout is shown while maintaining the real proportions, and the red star indicates the position of valve “V5”.

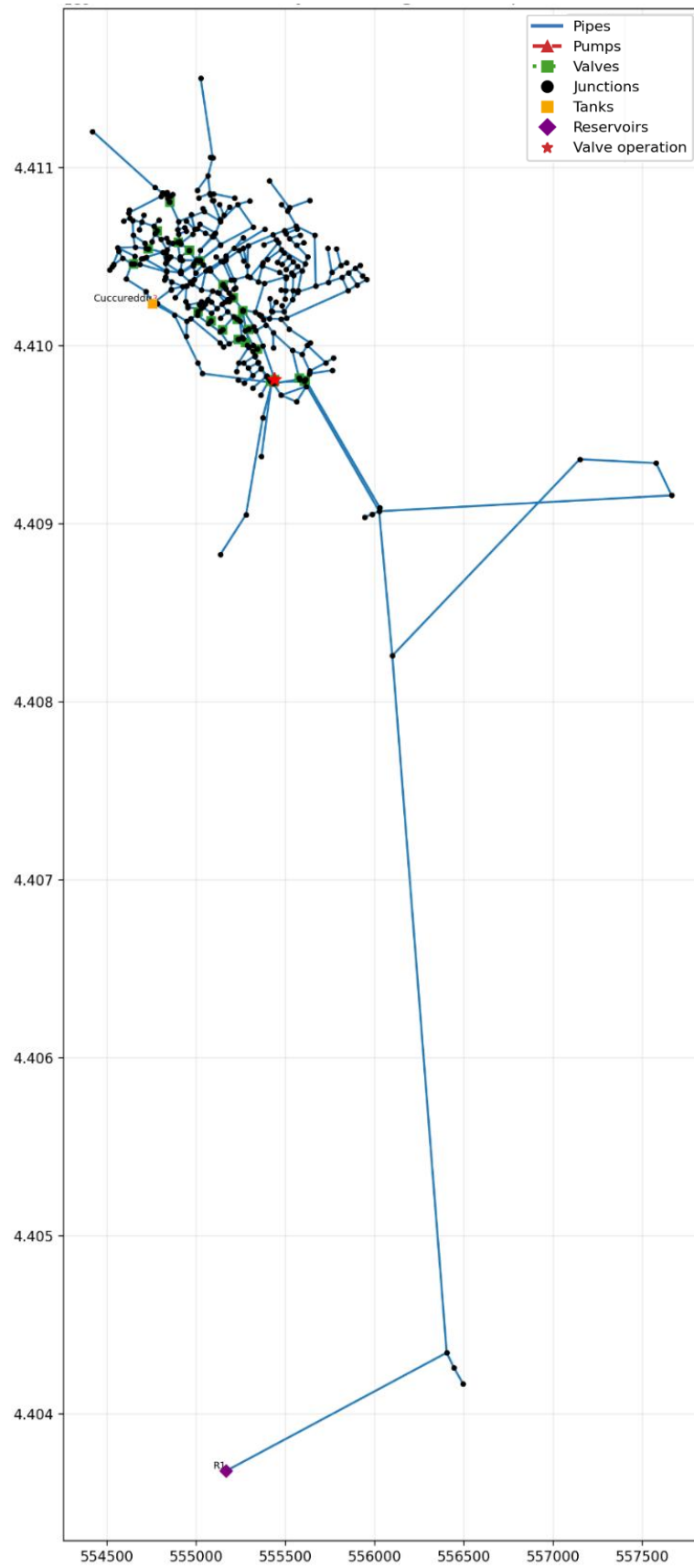


Figure 22: location of the maneuver of valve “V5” shown with the red star

To intuitively visualize the effects produced by the closure of the valve on the network, the graphs (figures 23 and 24) show a colormap of the maximum pressures reached in the distribution network corresponding to the urban area of Bari Sardo, one for each of the two scenarios.

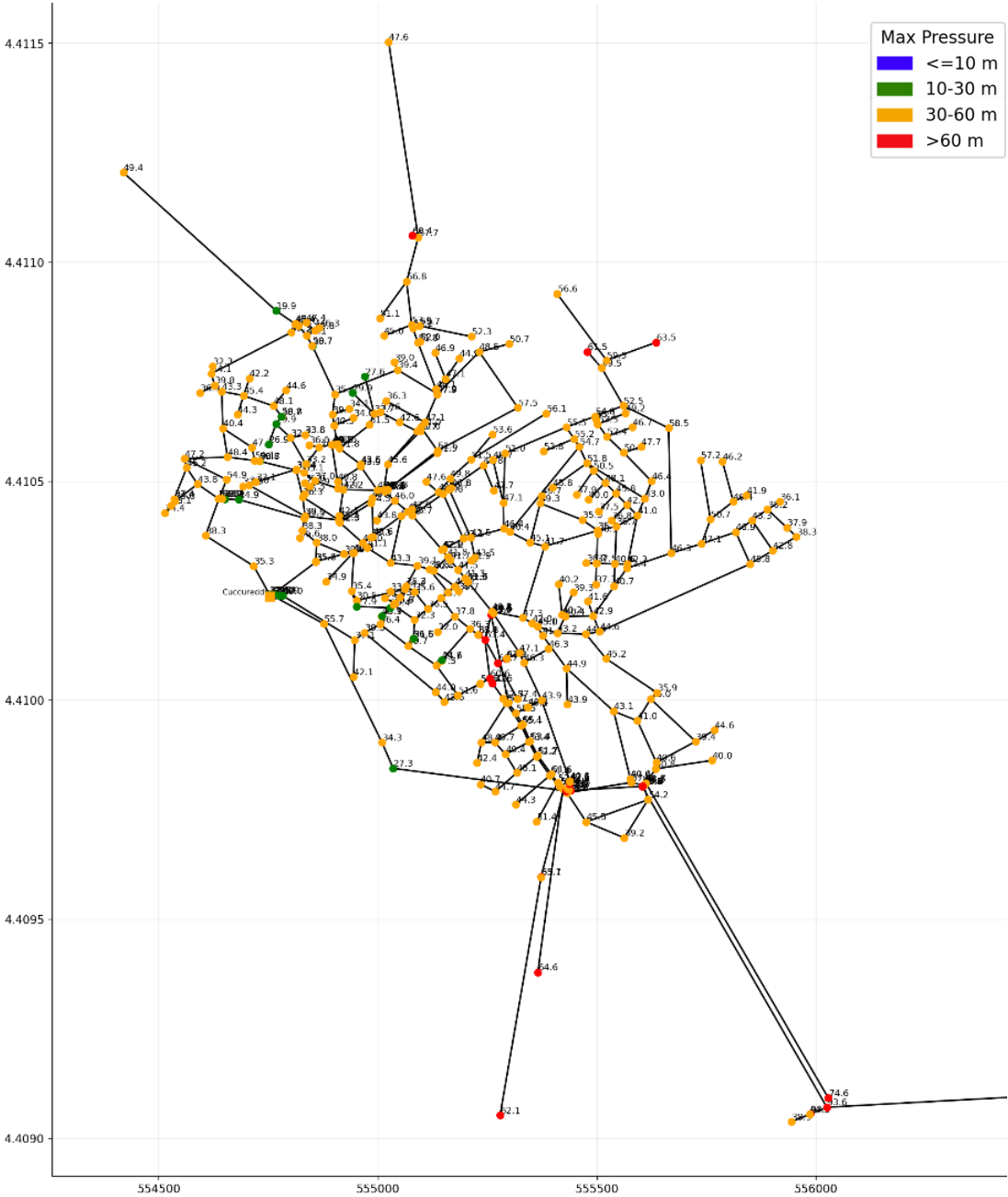


Figure 23: colormap of maximum pressure for each node in summer – $Q = 20$ l/s

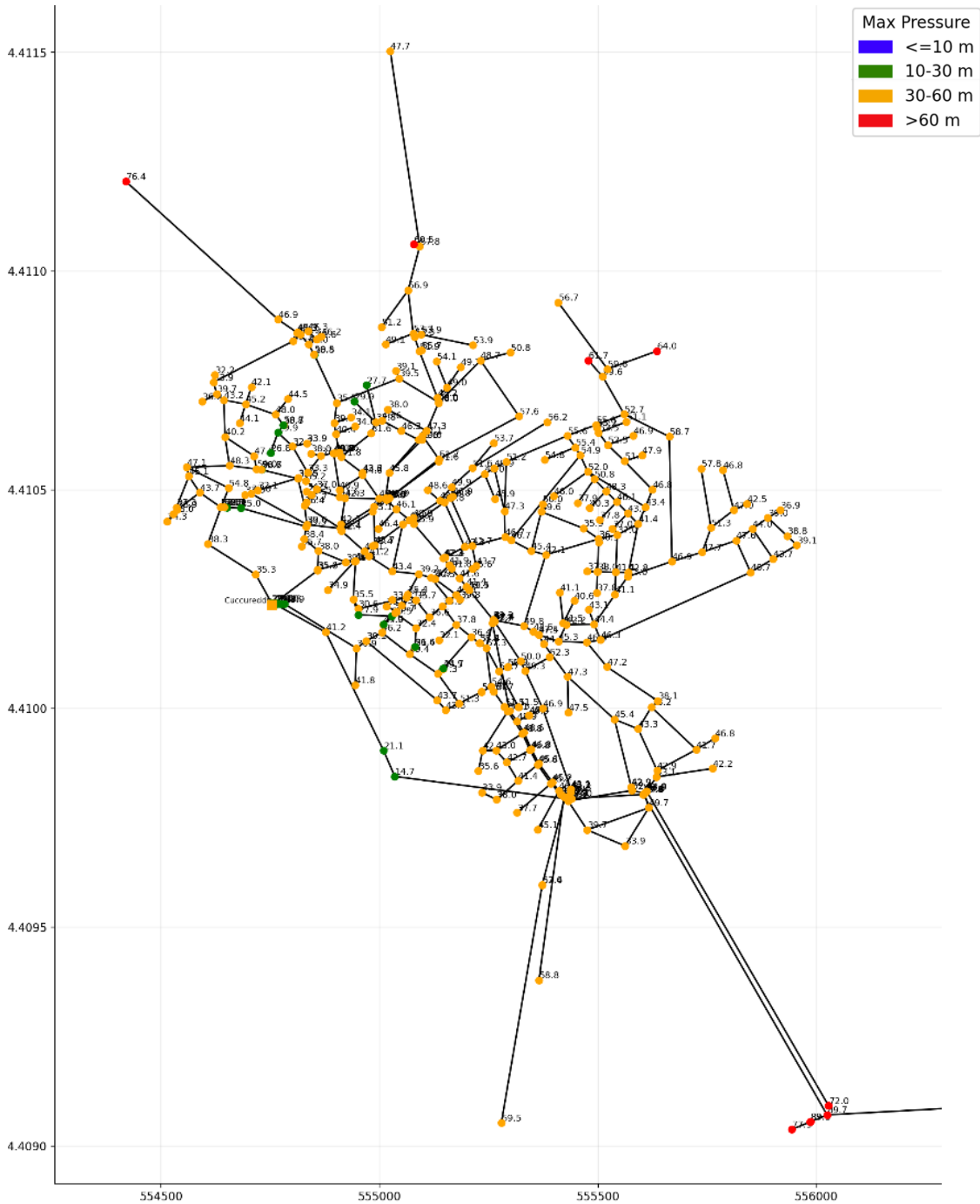


Figure 24: colormap of maximum pressure for each node in summer – $Q = 50$ l/s

Observing the two graphs, it can be noticed that in the scenario with lower flow rate higher pressures (highlighted in red) are reached in the distribution network, whereas in the scenario with higher flow rate higher pressures are reached in the adduction line. It

should be noted that the pipes set as closed in the EPANET model were not represented in the maps.

The following graphs (figures 25 and 26) instead highlight in red the nodes where negative pressure occurred.

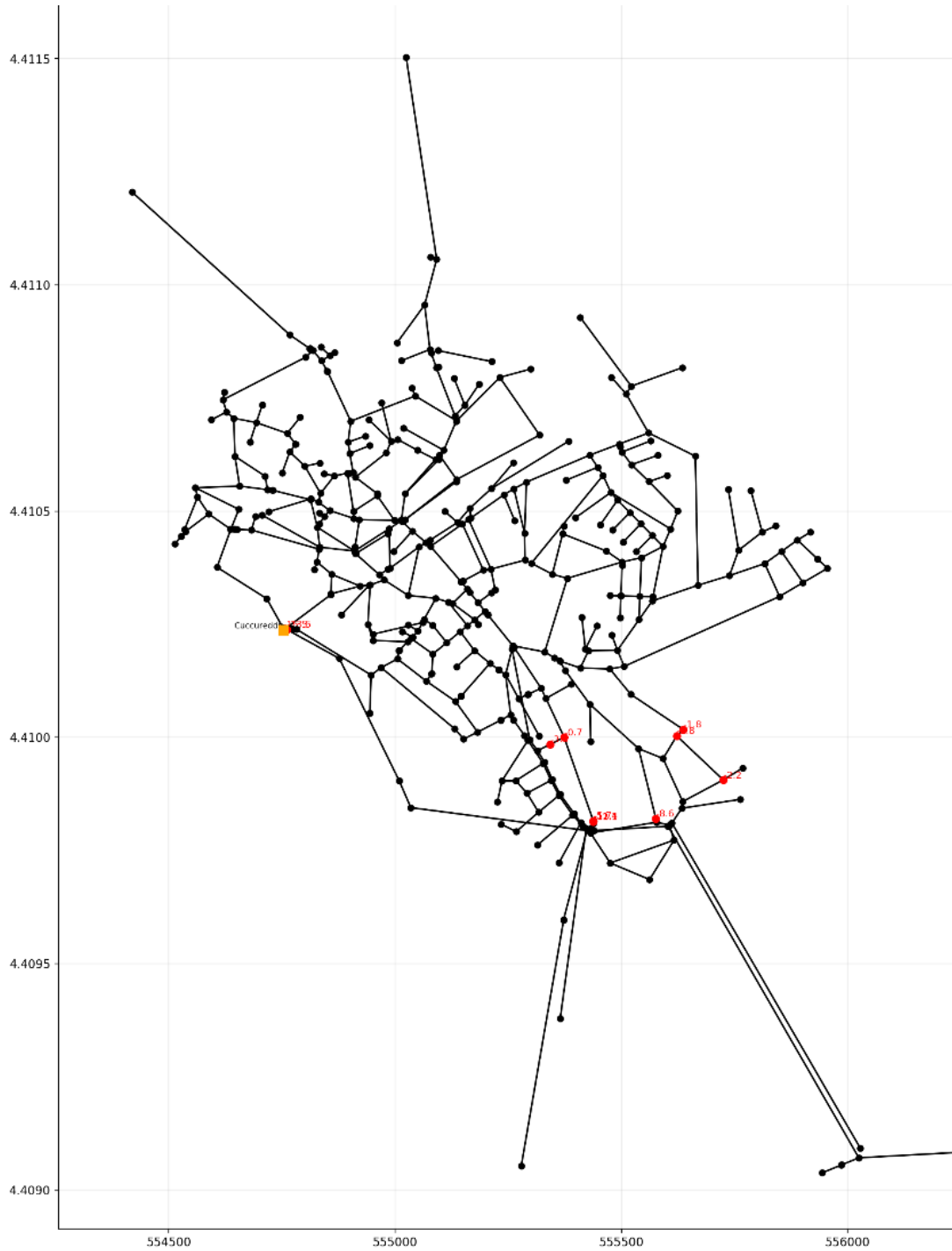


Figure 25: map of minimum pressure for each node in summer – $Q = 20 \text{ l/s}$

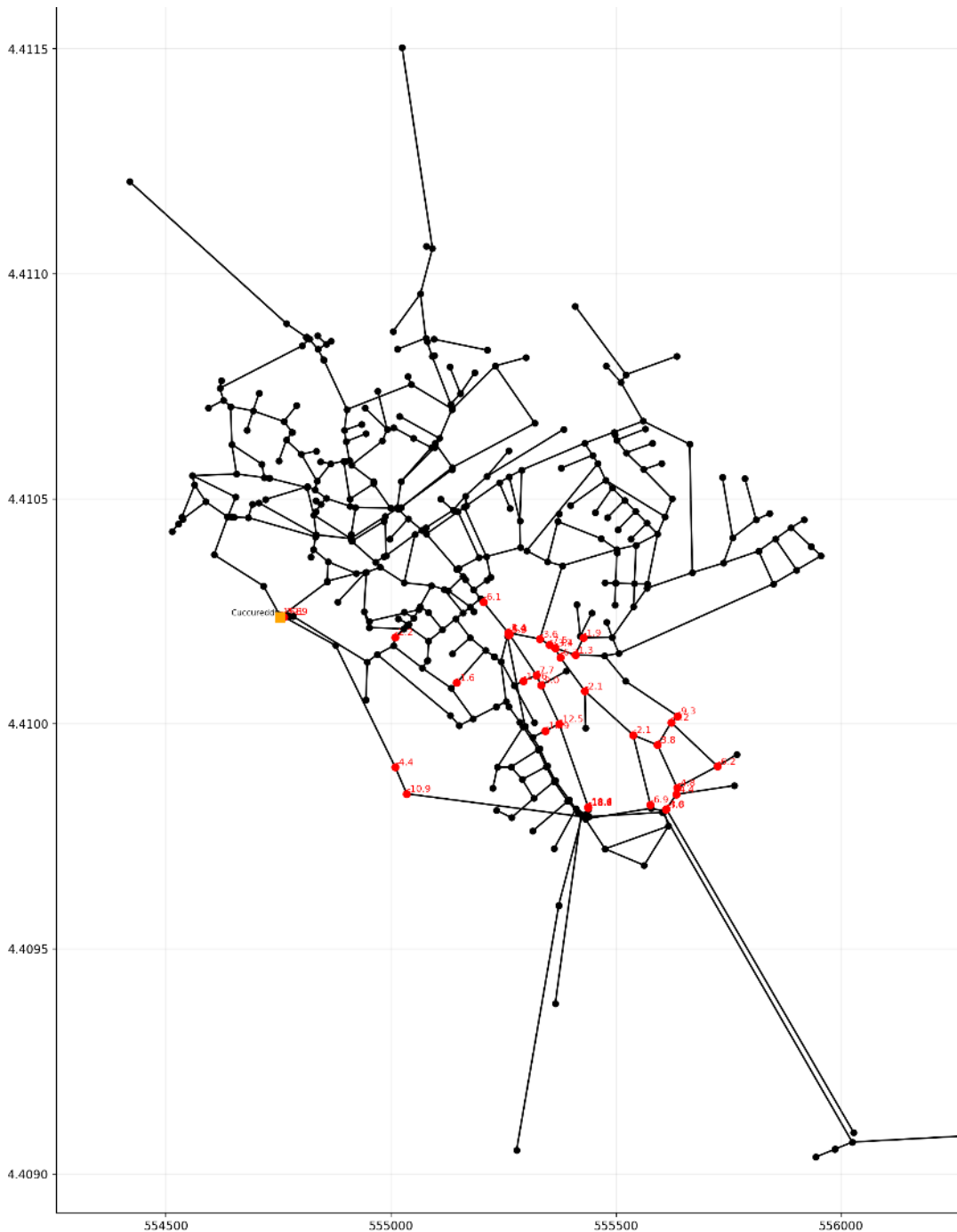


Figure 26: map of minimum pressure for each node in summer – $Q = 50$ l/s

By comparing the graphs between the two scenarios, it is evident that in the scenario with higher flow rate negative pressures occur in many more nodes. In both scenarios, however, the junctions reaching negative pressure are concentrated in the southern part of Bari Sardo, which also suffers from low pressure under steady-state conditions.

Moving to the analysis of the time series, the first ones refer to the node upstream of gate valve “V5” and are reported in graph below (figure 27).

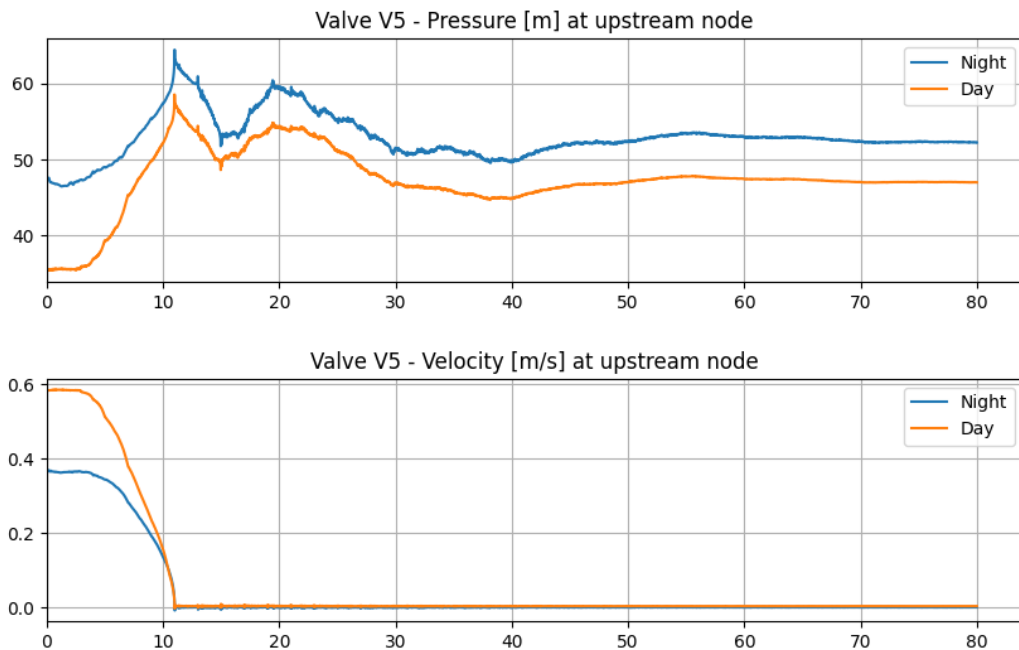


Figure 27: time series at the upstream node closing valve "V5"

The behavior observed is the typical one for a node upstream of a valve: at the end of the closure an increase in pressure occurs and, subsequently, an oscillatory behavior is observed until a new equilibrium is reached. In fact, the oscillation takes about 20 seconds to damp out and stabilizes at a value slightly higher than the initial one, which remains constant until a new perturbation of the system occurs. This value is the same that would be obtained from EPANET if the steady-state calculation were repeated with the valve closed.

From the comparison of the two scenarios it can be observed that in the nighttime case (blue line) the initial pressure is slightly higher than in the daytime case (orange line), and the oscillation behavior is approximately the same, except for the pressure behavior during the closing phase. Observing the time series of velocity, it can be noted that, consistently with the pressure behavior, the velocity decreases to zero at the end of the closure.

Graph (figure 28) instead shows the time series related to the node downstream of valve “V5”.

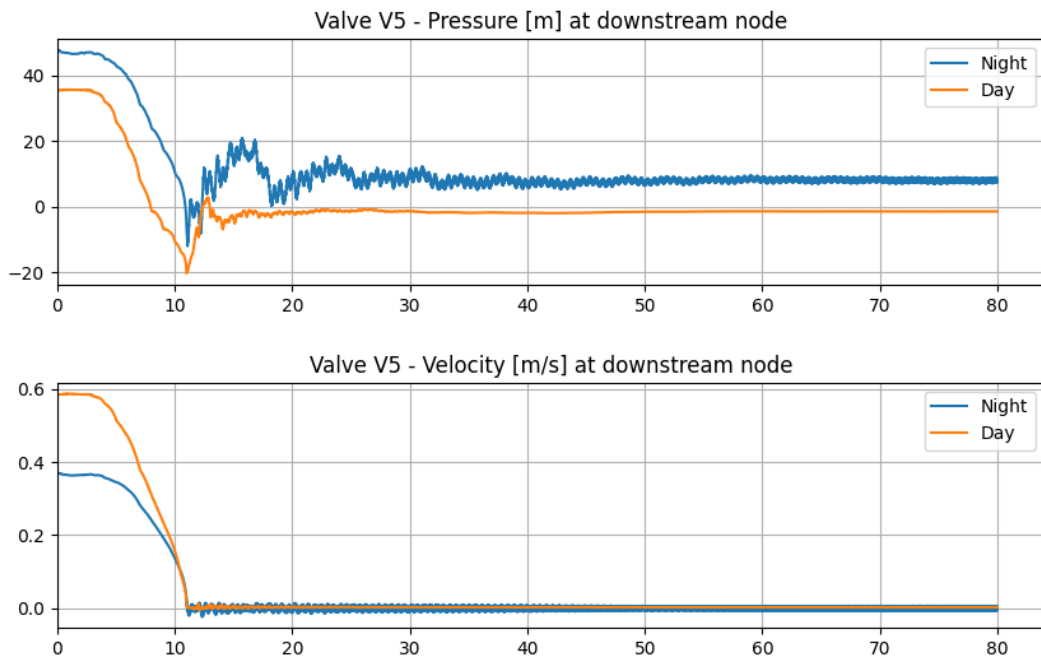


Figure 28: time series at the downstream node closing valve "V5"

In this case an opposite behavior to the previous one is observed: at the end of the valve closure a pressure drop first occurs, reaching about -20 m, followed by oscillations until the new steady state is reached. As in the previous case, except for a discrepancy during the maneuver, the effects produced by the maneuver in the two scenarios show a similar behavior.

It can be noted that in the nighttime scenario the damping is slightly slower than in the daytime scenario, since the oscillations are more pronounced. However, the most important information concerns the minimum values reached, which represent a critical condition for the network and are more dangerous in the daytime scenario.

Finally, the time series related to node “J7” (figure 29), where the maximum pressure occurs as previously discussed, can be compared. This junction is located on the adduction line, therefore the initial pressure is already high compared to the nodes of the distribution network.

As in the previous graphs, the trends are very similar and vertically shifted by a certain value. It is interesting to observe that while for the nodes upstream and downstream of the valve the pressure peak occurs after 11 seconds from the beginning of the simulation, in this case the peak occurs after about 16 seconds. The reason is that node “J7”, being located about 6 km away from valve “V5”, is reached by the pressure wave which travels at 1200 m/s after approximately 5 seconds.

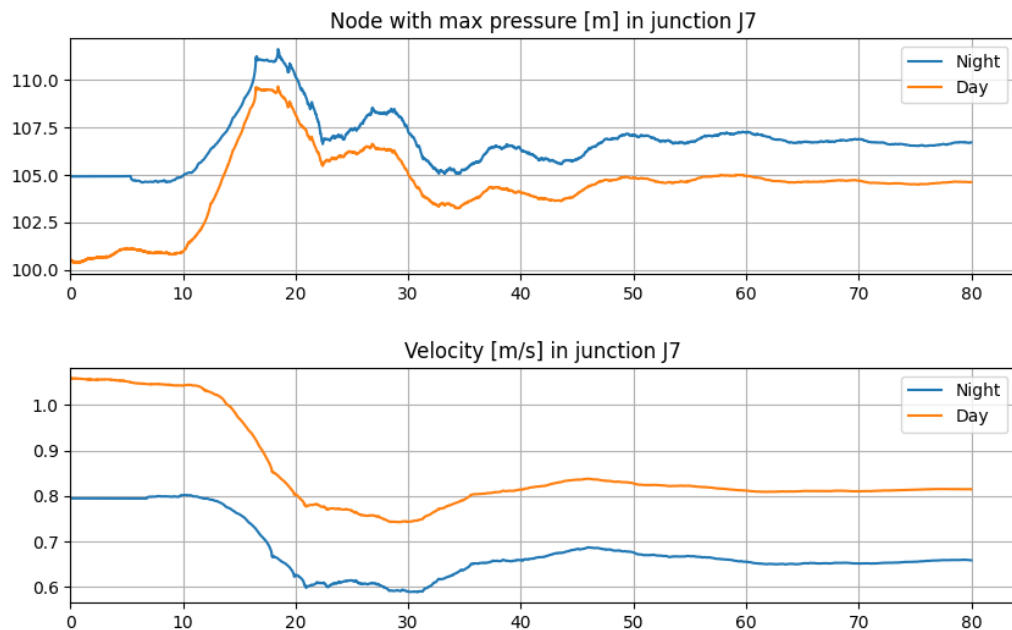


Figure 29: time series at node "J7" closing valve "V5"

The time series of the node where the minimum pressure occurs coincide in this case with the node downstream of the valve, therefore reference should be made to the graph in figure 28. It should be noted that for the selection of the minimum pressure the node downstream of the FCV “V2” was not considered, although it reaches even lower pressures. This node is influenced by the effect of the FCV, which is an artificial device used to regulate the flow during the simulations and is not foreseen in the actual project. For this reason, the node downstream of valve “V2” was not considered.

5.4 Autumn scenarios

In the autumn scenario, due to the decrease in tourists and the consequent reduction in demand, the pump is switched off, bypass “B” is closed by the gate valve “V5”, and

bypass “A” supplies only the Gramsci district, isolating it by closing valve “N1”. The rest of the network is therefore supplied by gravity from the Cuccureddu tank. Consequently, the valves that remain open are “V6”, “V22”, and “V47”. As in the summer case, a map showing the layout of the open and closed valves is reported.

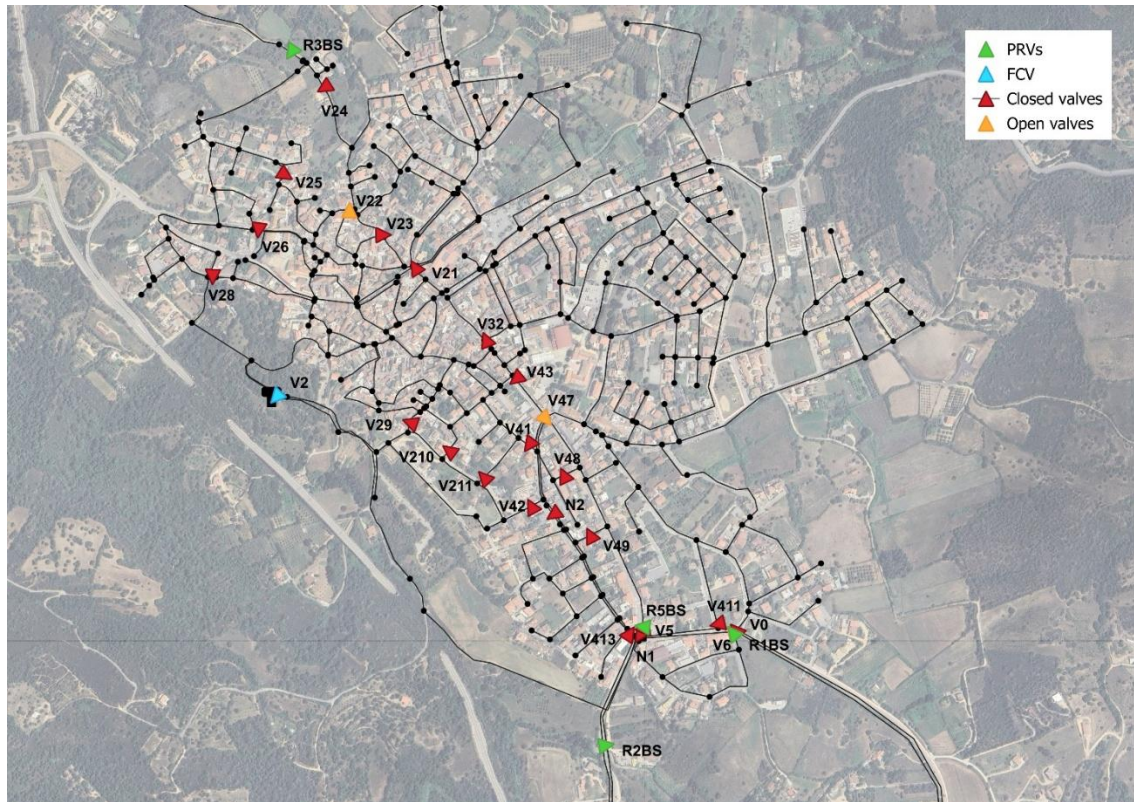


Figure 30: gate valves status in autumn configuration

As in the summer case, the two analyzed scenarios consider 20 l/s demanded from the network during the day and 10 l/s during the night. The outflow from the Genna Masoni reservoir reaches 40 l/s. Since during this period of the year the demand is lower and bypass “B” is closed, a greater flow rate can be conveyed to the Cuccureddu tank compared to the summer scenario. Through valve “V2”, an inflow of 25 l/s to the reservoir was set, which must guarantee the water supply for almost the entire network. The maps below (figures 31 and 32) show the valve status during the autumn period and the enlargement near the two bypass branches.

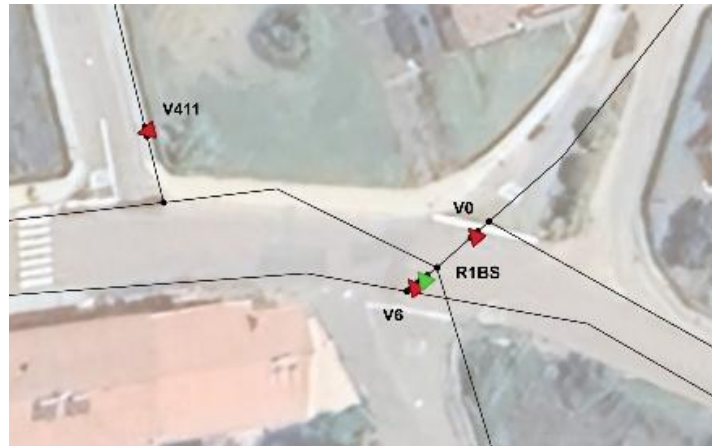


Figure 31: enlargements of bypass “A”

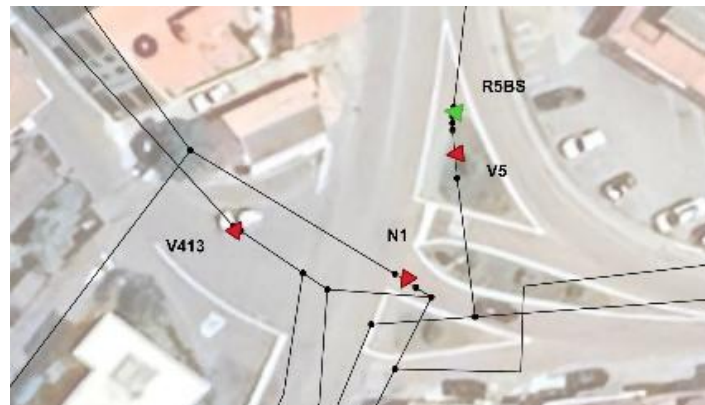


Figure 32: enlargements of bypass “B”

5.4.1 Results for autumn scenarios

Also for the two autumn scenarios, the results of the simulations were reported in specific histograms in order to clearly visualize the consequences of the performed maneuvers. Figure 33 shows the maximum pressures that occurred, and it can be observed that both for the closures and for the openings the maximum pressure always occurs at node “J7”, located on the adduction line. As discussed for the summer case, this means that no higher pressures are generated in any node of the distribution network. In the autumn scenarios, however, a worse maneuver cannot be distinguished with regard to the maximum pressures. Comparing the two simulated scenarios instead, the case with lower demand flow shows slightly higher pressures, as also happens when comparing the summer scenarios.

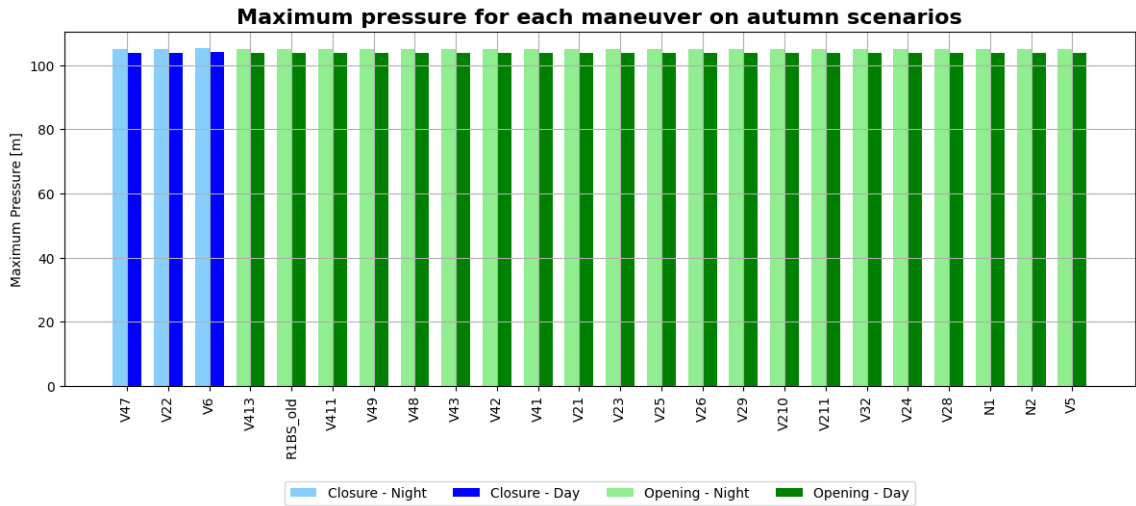


Figure 33: : histogram of maximum pressures for each maneuver in autumn scenarios

By analyzing the histogram (figure 34) related to the minimum pressure reached for each maneuver, it emerges that, as in the summer scenarios, closures generate a more intense water hammer. The only difference is that in this case the opening of valve “V5” generates a pressure slightly below zero, equal to -0.5 m.

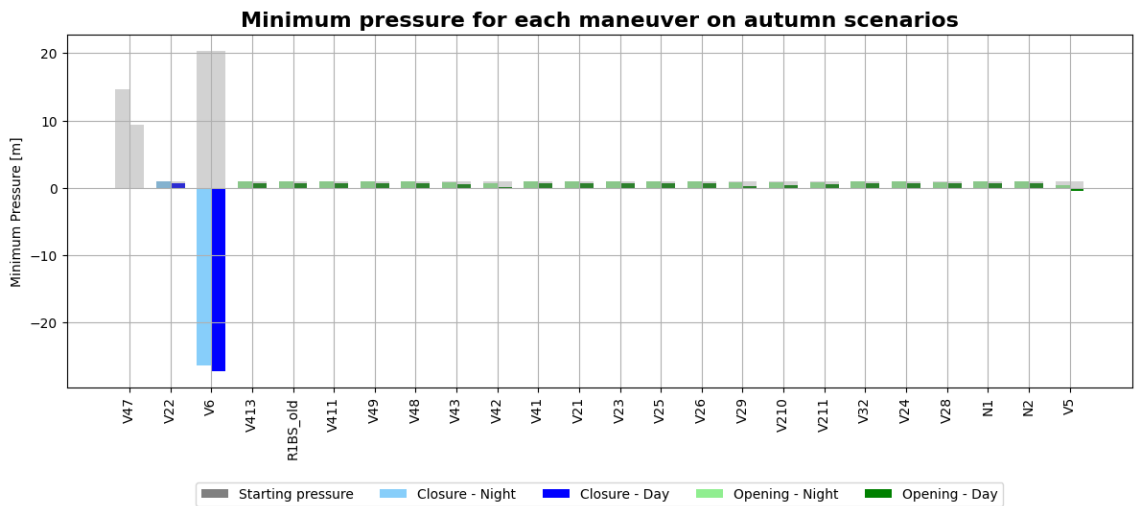


Figure 34: : histogram of minimum pressures for each maneuver in autumn scenarios

The closures instead show very low values and, in the case of valve “V47”, the pressure stabilizes at zero. In reality, this is neither a consequence of the water hammer nor a

calculation error, but it depends on the topology of the network. To explain this behavior, valve “V47” is taken as an example, whose position is shown in figure 35, and the elevations reported at each junction are observed.



Figure 35: part of Gramsci district with the elevation in [m] for each node

The pipes highlighted in red connect nodes that are supplied only when gate valve “V47” is open, since gate valves “N1” and “V413” are closed. When “V47” is also closed and the network tends toward a new equilibrium condition, the pipes drawn in red form a closed circuit that therefore no longer communicates with the rest of the network.

Consequently, the minimum pressure, which occurs at node “P5” highlighted in red, is a value determined by the equilibrium condition toward which the system tends and is not caused by water hammer.

Since it is an isolated circuit, the hydraulic head is no longer governed by the Cuccureddu tank, which becomes disconnected, but is determined by the node at the highest elevation, which is node “P5”, as occurs in hydrostatic conditions. Therefore, according to this logic, node “P5” has a hydraulic head equal to the elevation of 70.20 m a.s.l. and a pressure of 0 m. The time series of pressure and velocity at this node are reported below (figure 36).

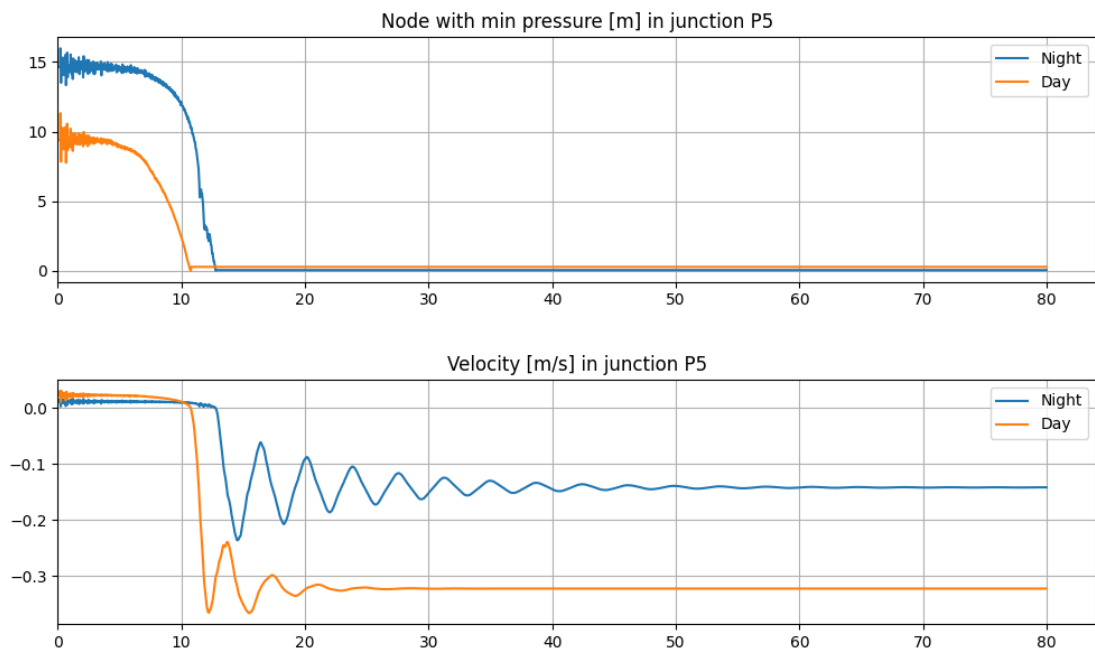


Figure 36: time series at node "P5" closing valve "V47"

At the node downstream of valve “V47”, the pressure toward which the system tends for equilibrium follows the same reasoning. Since the elevation is 47.22 m a.s.l. and the hydraulic head is determined by node “P5”, the pressure downstream of the valve is obtained simply by taking the difference between the two values, obtaining approximately 23 m. This value is consistent with the results obtained from the simulations, as can be observed from the time series calculated downstream of valve “V47” (figure 37).

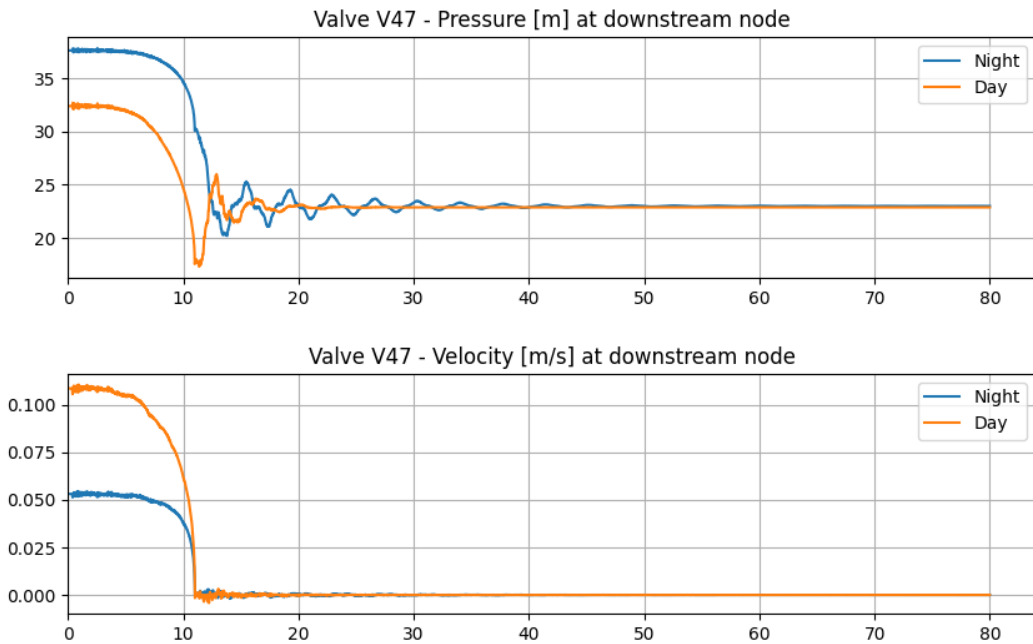


Figure 37: time series at the downstream node closing valve "V47"

The exact same phenomenon occurs for valve “V6”, since in this case as well, by closing the gate valve, the portion of the Gramsci district forms a closed circuit isolated from the rest of the network, which is therefore considered in hydrostatic conditions where the pressures are determined by the node belonging to the closed circuit located at the highest elevation.

As before, at the end of each simulation a summary table of the performed maneuvers containing the key values for each one is automatically produced. The summary tables for the autumn nighttime scenario ($Q = 10$ l/s) are reported in Appendix C, while those for the daytime scenario ($Q = 20$ l/s) are reported in Appendix D.

5.4.2 Detailed comparison of a opening maneuver

Since for the summer scenarios, for illustrative purposes, the complete discussion of a closure maneuver was reported, in this case it was chosen to report an opening maneuver, in particular the one applied to valve N1, which connects the two portions of the Gramsci district south of Bari Sardo. The position of gate valve “N1” is shown in figure 38.

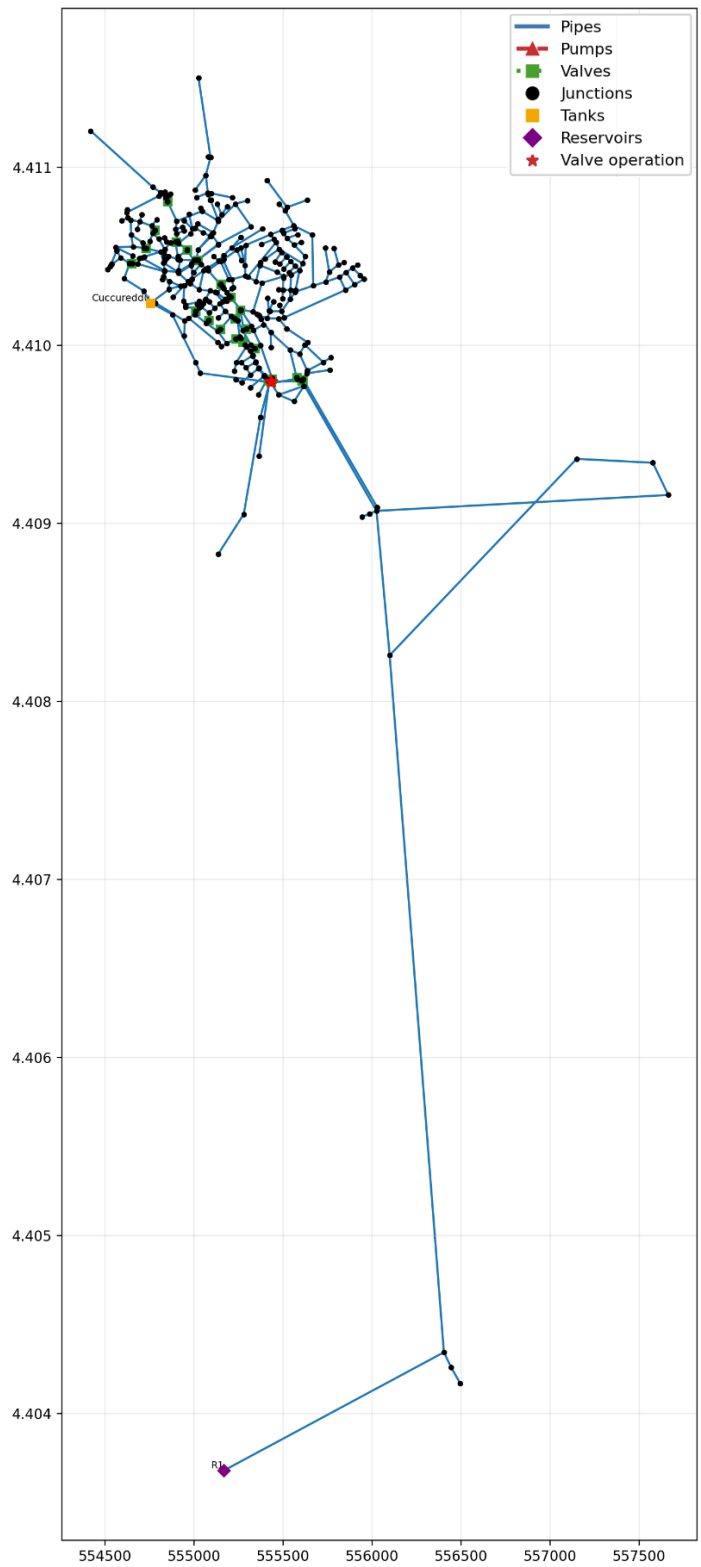


Figure 38: location of the maneuver of valve “NI” shown with the red star

In figures 39 and 40 the colormaps of the maximum pressure values reached at each junction in the two scenarios are again reported. It should be noted that compared to the

summer scenarios the pressures in the Cuccureddu alto district are lower since the pump is deactivated and the water supply comes exclusively from the Cuccureddu tank.

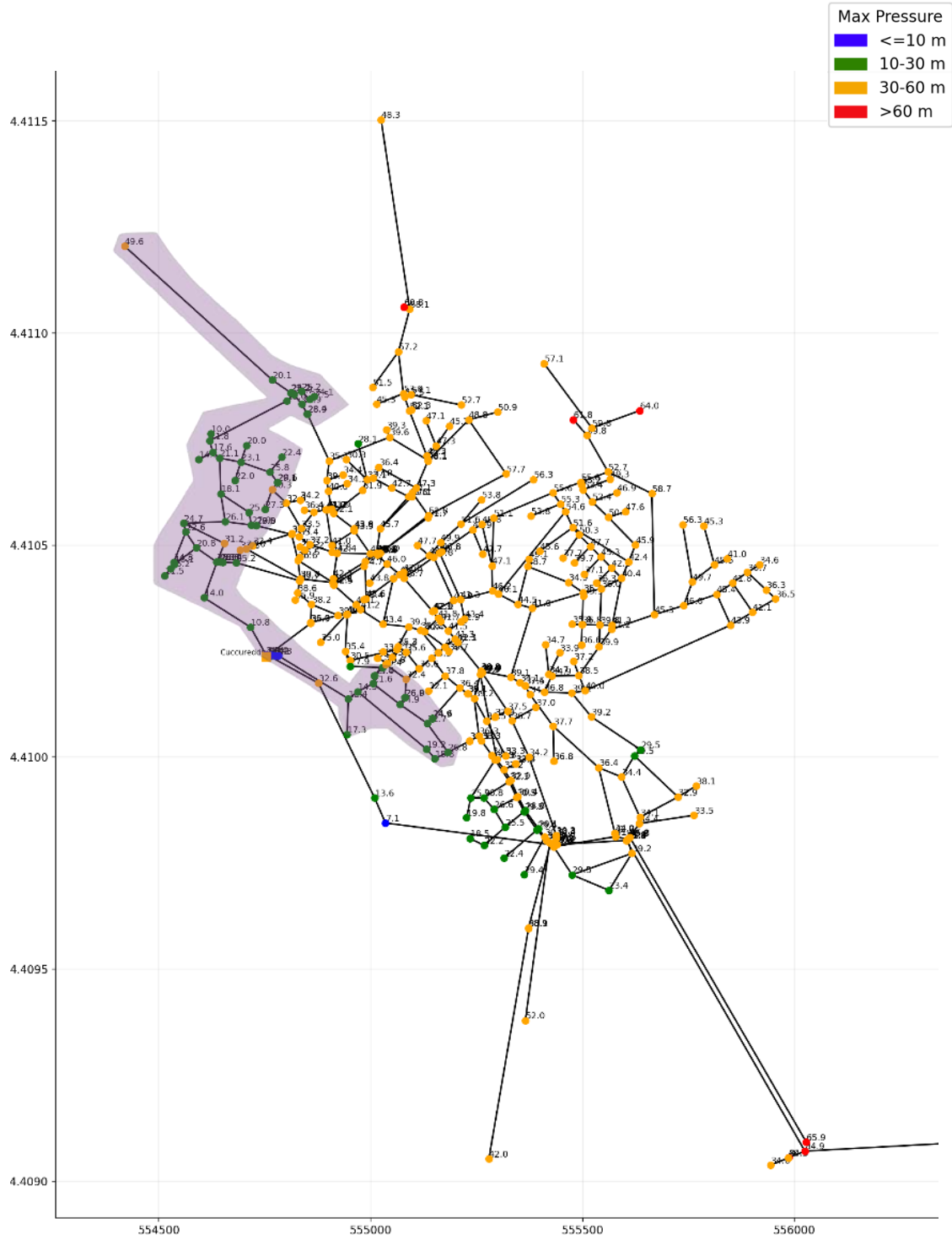


Figure 39: colormap of maximum pressure for each node in autumn – $Q = 10$ l/s; Cuccureddu alto district is highlighted in purple

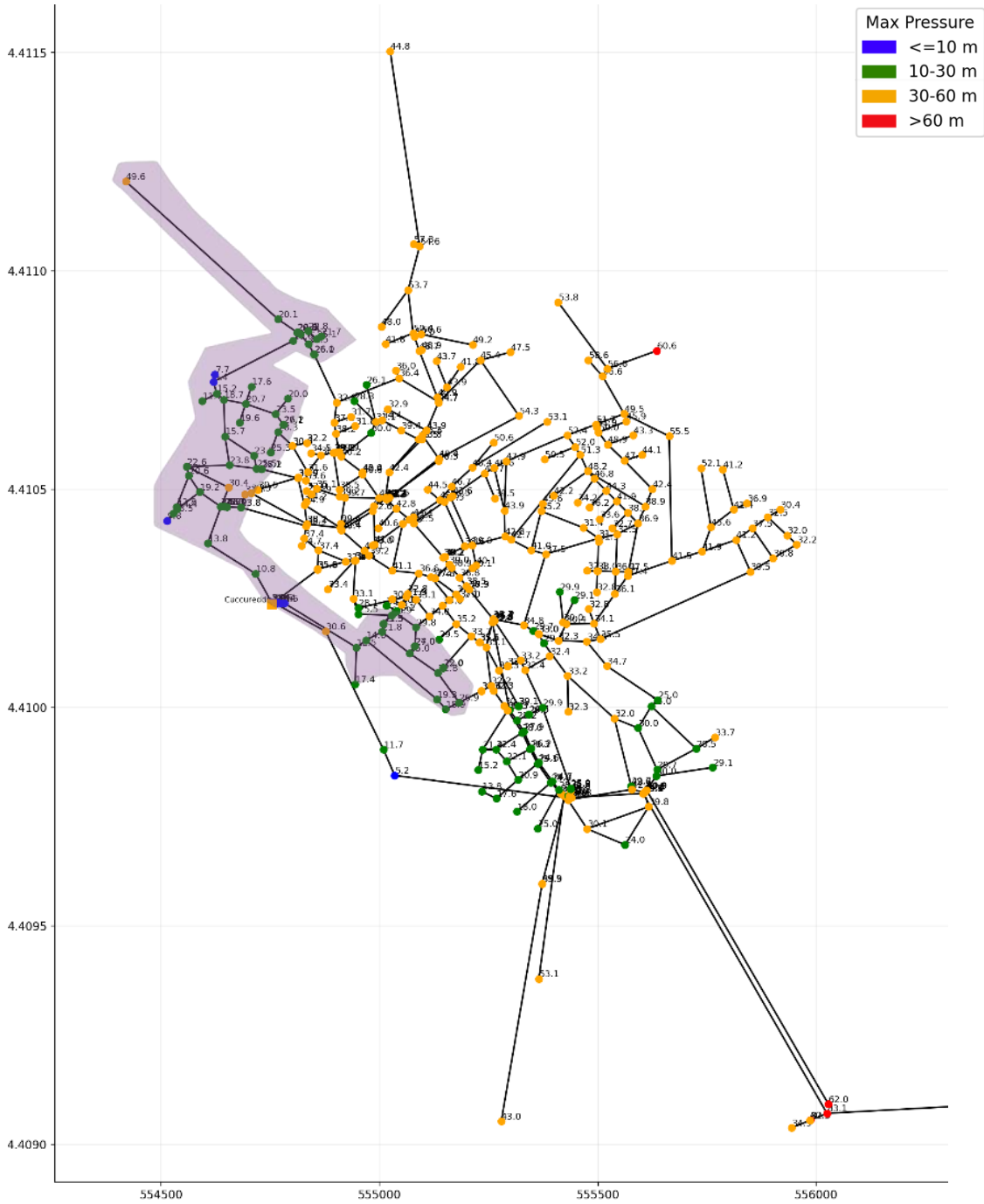


Figure 40: colormap of maximum pressure for each node in autumn – $Q = 20$ l/s
Cuccureddu alto district is highlighted in purple

The map representing negative pressures is not reported because the selected maneuver does not generate any pressure below zero.

Below, the time series obtained at the upstream and downstream ends of the valve are first reported. Figure 41 shows the temporal evolution upstream of the valve, where a gradual decrease in pressure during the opening can be observed. Neither of the two scenarios presents significant oscillations and they differ only in the value to which they converge in order to establish the new equilibrium, since it depends on the demand flow from the network.

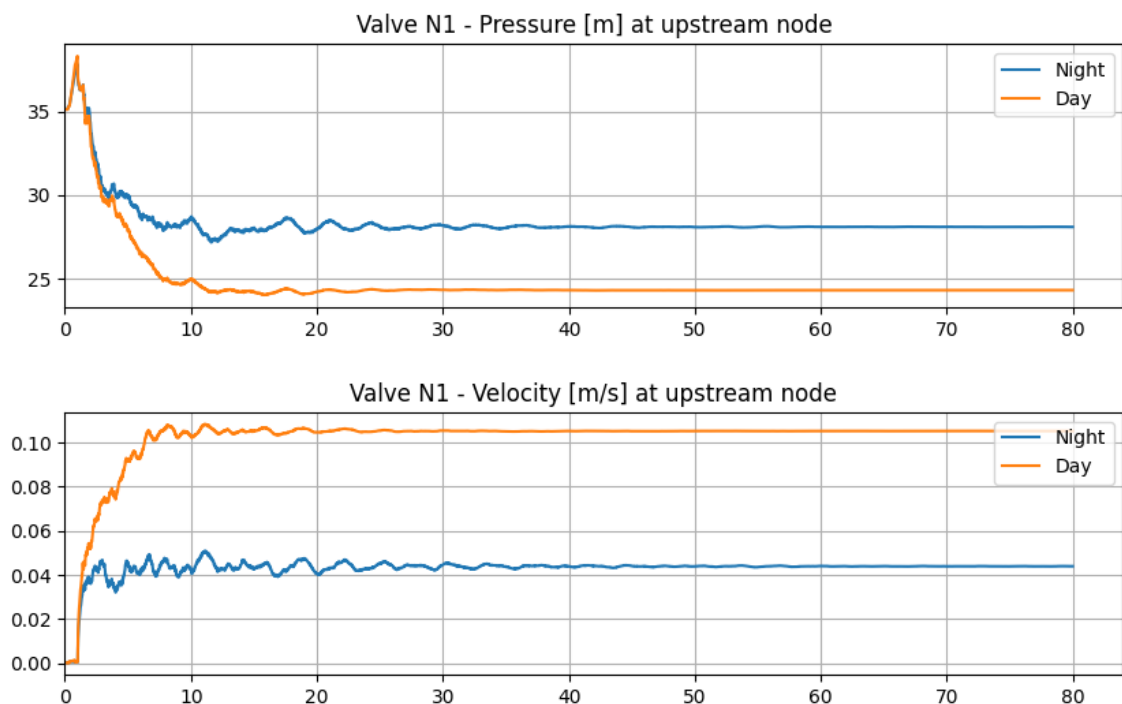


Figure 41: time series at the upstream node opening valve "N1"

Subsequently, the temporal evolution of pressure and velocity downstream of the gate valve is reported in the graph below (figure 42). As in the previous case, the low intensity of the water hammer does not generate significant oscillations and the pressure trend in the two scenarios is almost identical but vertically shifted by a few meters depending on the flow rate. Consistently with the demand multiplier values used in the two scenarios, which are one double the other, the velocity reached at convergence maintains the same proportionality ratio.

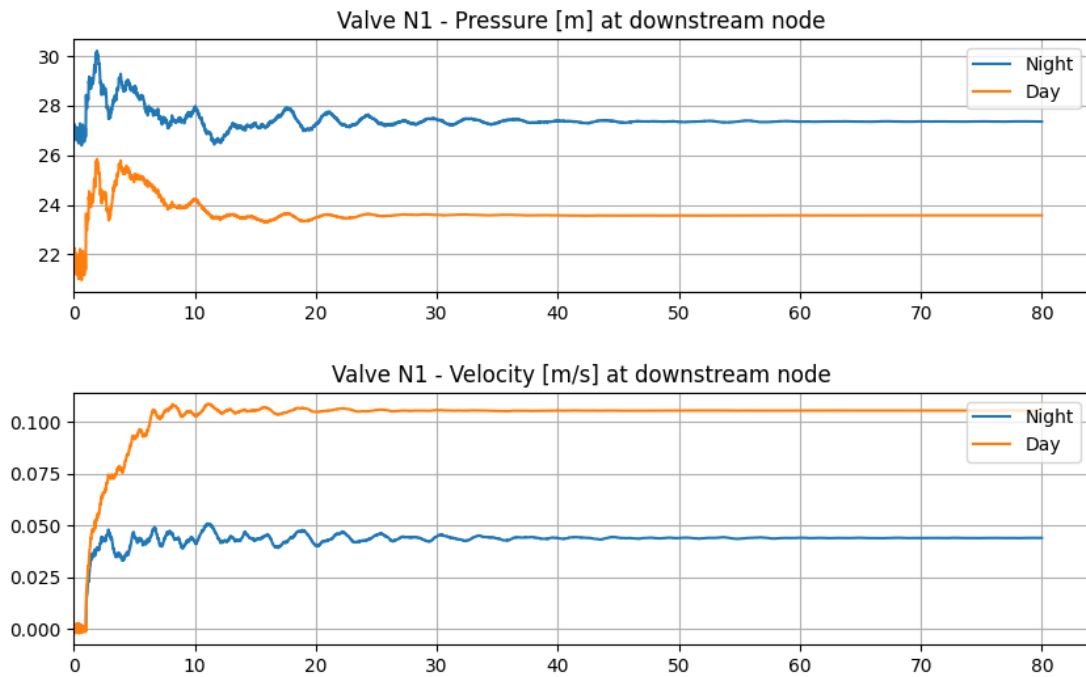


Figure 42: time series at the downstream node opening valve "N1"

By analyzing the maximum pressure reached in the network, the highest value occurs at node "J7", located on the adduction line, as in the summer case. The temporal evolution of the examined variables at node "J7" is reported in the following plot (figure 43). The pressure wave generated by the maneuver travels approximately 6.5 km to reach node "J7"; in fact, as can be seen from the graph, the observed effect is visibly damped and almost negligible.

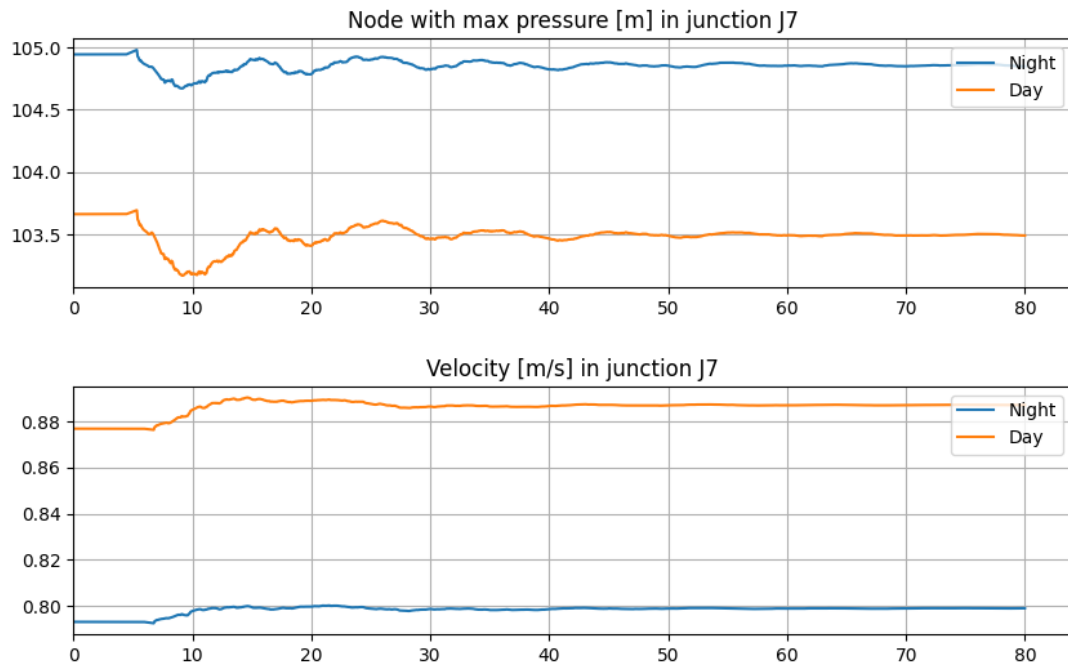


Figure 43: time series at node "J7" opening valve "N1"

Finally, the time series for node "4", where the minimum pressure occurs following the maneuver, are reported in figure 44. This node is located immediately downstream of the pump installed after the Cuccureddu tank, which, being turned off, does not provide pressure support to the nodes located after it. For this reason, the pressure at junction "4" is close to zero. It should be remembered that the elevation of the Cuccureddu tank is 83 m a.s.l., while that of node "4" is 85.5 m a.s.l.. Although it is higher, the pressure is positive because the elevation of the tank must be added to the height of the free water surface stored inside it, which can reach a maximum of 4 m.

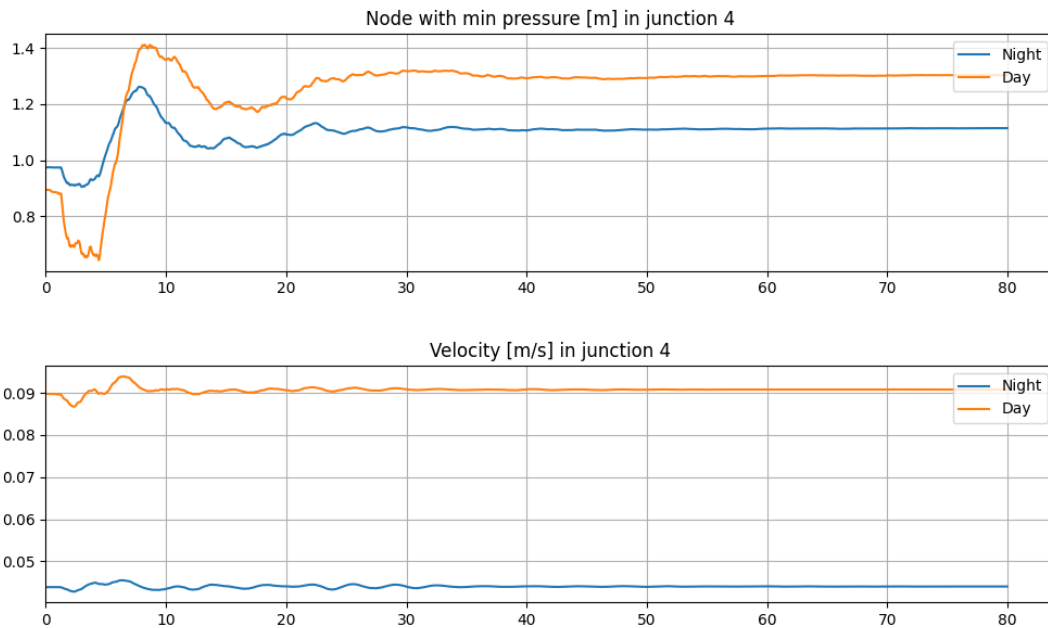


Figure 44: time series at node "4" opening valve "N1"

5.5 Safety checks and protection devices

In light of the results obtained, it is observed that the maximum pressures reached in the network are similar across the four scenarios, except for the nodes in the Cuccureddu alto district, which reach approximately 20 m higher pressure during summer due to the pump. Regarding negative pressures, it is evident that the closing maneuvers in the summer scenarios are the most critical.

From these observations, two checks follow that must be carried out to operate safely in the network. The first check is aimed at ensuring that the maximum pressure reached in the pipes does not exceed the maximum tensile strength of the material from which the pipes are made. The network is composed of steel, cast iron and polyethylene (PE) pipes. For cast iron and steel pipes, the admissible operating pressure (PFA) is generally between 30–40 bar and 40–60 bar respectively. Since in the network, also considering the pressures reached in the adduction pipeline, values are always below 110 m, which corresponds to 11 bar, they remain well below the limiting strength of the material.

For PE pipes, however, it is not immediate to verify their adequacy and it is necessary to use the Mariotte relation.

$$\sigma = \frac{r * p}{e} \quad \text{Mariotte's relation} \quad (37)$$

PE pipes are labeled as PE-xx where xx indicates the maximum tensile strength of the material. In the Bari Sardo water supply system there are pipes ranging from PE32 with a diameter of 26 mm to PE110 with a diameter of 90 mm.

It should be noted that from Mariotte's relation the maximum tensile strength of the material σ is directly proportional to the internal radius r and inversely proportional to the thickness e .

Taking PE32 pipes as an example, it is good practice to consider a safety factor, for example 1.5, before proceeding with the inverse formula of equation (37) by explicitly expressing p . Replacing σ with the value $3.2/(1.5)$ MPa, assuming a thickness of 4 mm and consequently an internal radius of 12.2 mm, it is obtained that the PFA is equal to 0.7 MPa, that is 70 m.

The same calculation was carried out for each type of PE pipe, obtaining very similar PFA values. PE pipes were used only in some sections of the distribution network. As mentioned during the study, in the summer scenarios the maximum pressure reached in the network is about 74 m. This value is very close to the resistance calculated with a safety factor equal to 1.5.

It can therefore be deduced that the system is formally at the limit of safe operation, but it is important to consider that operating so close to the PFA reduces the useful life of the material. In the presence of leaks or local weaknesses in the pipe, the risk of pipe rupture increases, making these sections of pipeline vulnerable.

The second check to be carried out concerns negative pressures, which must absolutely be avoided in order to prevent cavitation phenomena or pipeline implosion. Figure (45) shows a collapsed section of a pipeline, which has been irreparably damaged from negative pressure caused by water hammer.



*Figure 45: collapsed pipe due to water hammer
(source: Harper Haines website)*

To reduce and counteract the effect caused by the occurrence of negative pressures, several solutions can be adopted. One possible solution consists of performing the valve closing maneuvers more slowly. In fact, increasing the closing time leads to a lower intensity of water hammer and of the resulting effects.

Pipeline implosion occurs when the exchange of air with the external environment is not allowed; when a negative pressure is generated, the pipe tends to draw air from the outside, but if this is not possible it collapses on itself. For this reason, air valves are installed at critical points in the network, which allow the automatic management of the inflow or expulsion of air from the pipelines. They are generally installed in elevated areas of the network, at the ends of valves, and near slope changes, long pipeline sections, and flow meters.

Air valves are protection devices that exchange air with the outside depending on the situation. When a negative pressure is generated, due to water hammer or pipeline emptying, they allow the inflow of air in order to prevent the collapse of the pipes (figure 46).



*Figure 46: scheme of air valve that lets air in due to pipe emptying
(source: Vesipa R. Civil and industrial hydraulic systems – Lectures material, 2025)*

On the contrary, when a pipeline is being filled or when air bubbles are generated, they allow the expulsion of air (47).



*Figure 47: scheme of air valve that lets air out due to pipe filling
(source: Vesipa R. Civil and industrial hydraulic systems – Lectures material, 2025)*

Based on the analyses conducted on the Bari Sardo network, it emerged that node “P2” is a critical node in the steady state and potentially dangerous in the case of depressions caused by water, whose position was previously shown in figure (21). Furthermore, under conditions of high water demand, the pipes connected to this node could empty because in steady state conditions, the pressure approaches zero when the bypasses are open, thus not guaranteeing a constant water supply to the Cuccureddu tank.

This node is located at a higher elevation compared to the adjacent nodes because the pipeline follows the morphological trend which, in that area, is characterized by the presence of a hill. Being located before the Cuccureddu tank, only the effects of the maneuvers performed on the gate valves distributed in the network are damped by the tank; the maneuvers performed on the valves of bypasses “A” and “B”, instead, reach node “P2” without the damping effect provided by the tank.

From the documentation collected by the engineers of Studio Rosso Ingegneri Associati and provided by Abbanoa, an air valve is already installed in a nearby area. It represents a very effective position since it is a node located at high elevation and it’s connected by a pipeline with a steep slope. Therefore, it is essential to perform the necessary maintenance on the device in order to ensure its correct functioning.

5.6 Safe closure time evaluation

The results obtained for the closure of valve “V5” under the summer daytime scenario highlight a critical condition within the network. In particular, the pressure drops dangerously below zero during the transient phase and, even after the valve closure, it stabilizes at values close to zero. This behavior indicates that the network is operating under significant stress due to the high demand and is therefore unable to ensure adequate supply to all nodes.

For this reason, it is necessary to identify a solution that not only prevents the occurrence of negative pressures but also supports pressure levels in the nodes immediately downstream of valve “V5”, where the most critical conditions are observed. To solve this issue, the most critical operation within the most severe

scenario, which is the closure of valve “V5” in daily summer scenario, has been taken into account.

To avoid negative pressure, before closing valve “V5” it’s necessary to open other valves to sustain a positive pressure after its closing. To this purpose, a series of simulations was carried out closing valve “V5” after closing gate valves “V411” and “V49”. Moreover the calculation has been carried out with different time of closure, to achieve a more safe maneuver.

Closure times of 10, 20, 30, 40, seconds were considered, and the corresponding results are reported in the plot below (figure 48).

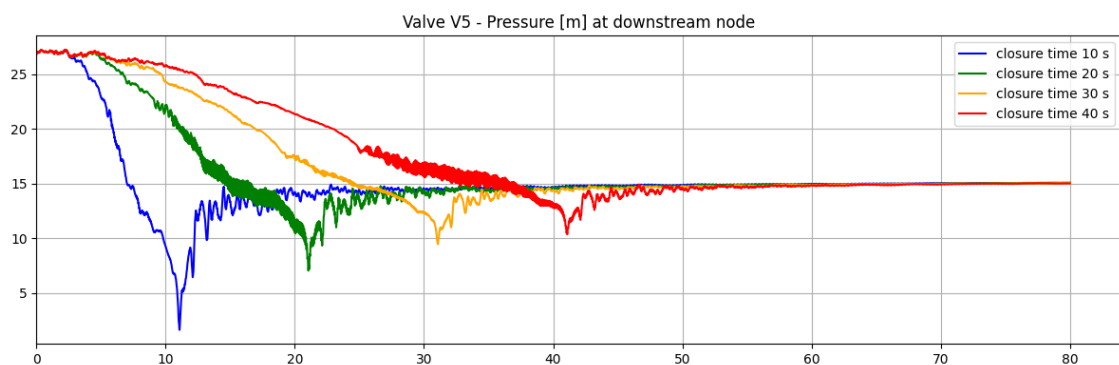


Figure 48: different closure time of valve "V5" after closing valves "V411" and "V49"

As can be observed from the graph, after opening valves “V49” and “V411”, even with a closure time of 10 seconds, the pressure does not drop below zero. Moreover, as the duration of the operation increases, the intensity of the water hammer effect decreases.

However, the minimum pressure remains very close to zero. For this reason, in order to ensure safer operating conditions, it’s better to perform the maneuver over a longer time, of at least 30 seconds. In fact, with a minimum closure time of 30 seconds, the pressure does not drop below 10 meters.

Conclusions

Through this thesis project, a method for the study of hydraulic transients applicable to networks of different complexity was developed by integrating a series of operations with the TSNNet and WNTR packages in order to generalize the method as much as possible. The study also demonstrates the potential of integrating open-source tools and numerical methods for the analysis of water hammer effects. In particular, attention was paid not only to obtaining a numerical solution, but also to a practical organization of the results and to generate graphs and maps to facilitate the interpretation of the results.

Through the described procedure, an example of application to the water supply system of the town of Bari Sardo was presented, making it possible to efficiently simulate several scenarios and provide a useful framework for identifying potentially critical operating conditions. The simulations were carried out for the four scenarios described, two summer and two autumn ones, considering different flow rates circulating in the network. The critical issues that emerged mainly concerned the closing maneuvers in the summer scenarios due to the occurrence of negative pressures. For reasons of length and readability, it was not possible to report in detail the results of all the maneuvers, but one closing and one opening maneuver were presented as examples.

This analysis also made it possible to assess a solution to prevent negative pressures in the network by adjusting the valve closure time, ensuring safe operating conditions.

Possible future developments of this work could include the integration of a correlation between the temporal evolution of hydraulic variables and topological characteristics in real networks, or the addition of the study of the effects caused by a pipe burst in addition to valve maneuvers.

In conclusion, the methodology presented in this study represents a tool applicable both to new water distribution network projects and to existing networks, useful for supporting the analysis and management of hydraulic transients in networks, contributing to safer operation and to the possible planning of safety improvement interventions.

Appendix A

Summary of pressure [m] for closure maneuvers - Q = 20 l/s scenario						
Valve ID	p _{max} UD	p _{max} DS	p _{min} UD	p _{min} DS	p _{max} network	p _{min} network
V22	42.99	42.25	40.09	30.56	104.96	9.78
N1	53.81	41.36	34.82	8.98	105.77	0
V5	64.44	47.58	46.45	-12.08	111.63	-12.08
V6	57.57	53.02	51.8	9.35	106.22	-9.35

Table 3: summary for closures in summer scenario - Q = 20 l/s

Summary of pressure [m] for closure maneuvers - Q = 20 l/s scenario						
Valve ID	p _{max} UD	p _{max} DS	p _{min} UD	p _{min} DS	p _{max} network	p _{min} network
V413	41.95	41.95	34.62	34.30	104.96	9.78
R1BS_old	44.98	43.29	39.98	41.60	104.94	9.76
V411	45.20	42.63	38.56	40.19	104.94	9.78
V49	44.32	42.76	37.42	41.35	104.96	9.78
V48	49.11	47.52	42.21	45.77	104.96	9.78
V47	49.98	50.32	48.48	44.81	104.95	9.78
V43	51.63	46.19	45.38	41.29	104.94	9.16
V42	58.03	53.21	52.31	38.78	105.31	9.78
V41	50.06	42.40	41.42	38.07	104.94	9.78
V21	45.61	45.58	45.13	45.09	104.96	9.78
V23	43.58	43.63	43.11	43.16	104.96	9.78
V25	50.71	35.37	34.93	28.68	105.07	9.78
V26	32.32	50.64	28.66	29.43	105.17	7.07
V29	47.92	29.39	24.79	23.91	105.27	7.89
V210	51.40	33.67	28.46	26.49	105.26	8.03
V211	49.47	38.79	37.41	24.50	105.11	9.78
V32	42.09	42.18	41.62	41.68	104.96	9.78
V24	35.30	50.53	28.37	32.23	105.08	9.78
V28	46.18	52.77	27.78	45.24	105.02	9.78
N2	46.21	48.26	38.94	40.98	104.97	9.78

Table 4: summary for openings in summer scenario - Q = 20 l/s

Appendix B

Summary of pressure [m] for closure maneuvers - Q = 50 l/s scenario						
Valve ID	p _{max} UD	p _{max} DS	p _{min} UD	p _{min} DS	p _{max} network	p _{min} network
V22	40.89	40.98	20.96	13.63	103.40	-11.48
N1	43.52	42.78	28.58	4.70	103.40	-11.47
V5	53.79	43.20	29.84	-18.90	108.49	-18.90
V6	49.02	48.93	36.39	4.53	103.40	-12.22

Table 5: summary for closures in summer scenario - Q = 50 l/s

Summary of pressure [m] for closure maneuvers - Q = 50 l/s scenario						
Valve ID	p _{max} UD	p _{max} DS	p _{min} UD	p _{min} DS	p _{max} network	p _{min} network
V413	43.62	43.65	43.10	43.13	103.42	6.50
R1BS_old	48.68	47.25	46.94	43.91	103.42	6.20
V411	47.26	46.18	44.92	42.91	103.42	6.42
V49	46.20	45.60	45.58	45.35	103.42	6.51
V48	50.92	50.30	50.14	49.98	103.42	6.51
V47	52.67	53.51	52.37	52.57	103.42	6.51
V43	54.50	48.42	47.08	41.38	103.42	1.61
V42	58.03	52.11	50.16	47.34	103.99	6.45
V41	52.53	46.93	45.09	38.16	103.42	5.40
V21	45.77	45.74	45.69	45.65	103.42	6.50
V23	43.72	43.76	43.59	43.69	103.42	6.50
V25	50.71	35.53	34.98	28.75	103.49	6.51
V26	32.39	50.64	28.73	29.23	103.57	6.51
V29	47.92	29.73	24.74	24.01	103.65	6.44
V210	51.40	33.96	28.40	26.59	103.66	6.46
V211	49.47	39.11	37.84	24.59	103.50	6.45
V32	42.22	42.38	42.12	42.15	103.42	6.50
V24	35.60	50.53	28.45	31.85	103.49	6.50
V28	46.06	52.77	27.87	45.54	103.45	6.49
N2	47.94	49.99	47.36	49.38	103.42	6.50

Table 6: summary for openings in summer scenario - Q = 50 l/s

Appendix C

Summary of pressure [m] for closure maneuvers - Q = 10 l/s scenario						
Valve ID	p _{max} UD	p _{max} DS	p _{min} UD	p _{min} DS	p _{max} network	p _{min} network
V47	40.49	37.83	37.31	20.20	105.06	0.00
V22	42.86	45.62	39.65	28.63	104.99	0.89
V6	53.42	52.00	51.31	-7.64	105.22	-26.34

Table 7: summary for closures in autumn scenario - Q = 10 l/s

Summary of pressure [m] for closure maneuvers - Q = 10 l/s scenario						
Valve ID	p _{max} UD	p _{max} DS	p _{min} UD	p _{min} DS	p _{max} network	p _{min} network
V413	31.19	37.74	26.22	27.42	104.98	0.91
R1BS_old	41.97	35.40	31.76	31.71	104.98	0.90
V411	42.70	34.60	31.20	31.09	104.98	0.91
V49	30.99	30.58	29.35	29.81	104.98	0.91
V48	35.31	35.27	34.80	34.83	104.98	0.91
V43	40.44	40.47	39.71	40.04	104.98	0.89
V42	33.16	32.78	32.14	31.37	104.98	0.67
V41	37.12	37.28	36.32	36.84	104.98	0.91
V21	44.61	44.58	44.53	44.50	104.98	0.91
V23	43.04	42.84	42.69	42.60	104.98	0.90
V25	28.29	28.29	28.21	28.22	104.98	0.91
V26	28.20	28.23	28.12	28.12	104.98	0.91
V29	23.05	23.63	22.50	23.13	104.98	0.82
V210	26.53	26.30	26.02	25.71	104.98	0.83
V211	24.60	24.53	24.15	23.77	104.98	0.83
V32	41.11	41.10	41.03	40.90	104.98	0.91
V24	28.08	28.05	27.90	27.84	104.98	0.90
V28	28.16	28.25	27.83	28.07	104.98	0.89
N1	37.82	30.21	27.17	26.40	104.98	0.90
N2	32.14	34.01	31.37	33.57	104.98	0.91
V5	45.97	41.48	39.80	27.45	104.98	0.36

Table 8: summary for openings in autumn scenario - Q = 10 l/s

Appendix D

Summary of pressure [m] for closure maneuvers - Q = 20 l/s scenario						
Valve ID	p _{max} UD	p _{max} DS	p _{min} UD	p _{min} DS	p _{max} network	p _{min} network
V47	37.57	32.70	32.12	17.31	103.96	0.00
V22	42.21	39.07	37.83	20.49	103.73	0.69
V6	52.27	50.02	49.11	-9.38	104.15	-27.28

Table 9: summary for closures in autumn scenario - Q = 20 l/s

Summary of pressure [m] for closure maneuvers - Q = 20 l/s scenario						
Valve ID	p _{max} UD	p _{max} DS	p _{min} UD	p _{min} DS	p _{max} network	p _{min} network
V413	28.54	38.23	20.10	23.97	103.69	0.69
R1BS_old	42.51	31.18	28.96	27.20	103.69	0.64
V411	43.01	31.04	27.60	25.61	103.69	0.69
V49	26.14	25.40	23.51	24.54	103.71	0.69
V48	30.20	30.08	29.54	29.57	103.71	0.69
V43	36.69	37.09	34.45	35.90	103.69	0.55
V42	33.05	30.62	30.07	26.04	103.69	0.04
V41	32.75	34.11	30.90	32.39	103.70	0.67
V21	40.86	40.83	40.75	40.71	103.71	0.69
V23	40.82	39.67	39.51	38.85	103.69	0.63
V25	25.95	26.04	25.73	25.77	103.71	0.70
V26	26.10	26.07	25.84	25.65	103.71	0.68
V29	22.94	21.89	20.56	20.10	103.69	0.25
V210	26.42	24.71	24.20	22.62	103.70	0.34
V211	24.49	23.77	22.79	20.57	103.70	0.47
V32	37.72	37.55	37.48	36.89	103.71	0.68
V24	25.24	25.54	24.65	24.93	103.72	0.68
V28	27.33	27.79	26.02	27.10	103.71	0.65
N1	38.31	25.85	24.03	20.97	103.69	0.64
N2	27.14	28.87	25.98	28.24	103.71	0.69
V5	44.00	39.75	37.92	22.17	103.69	-0.44

Table 10: summary for openings in autumn scenario - Q = 20 l/s

References

Technical reports and documentation provided by the engineering firm Studio Rosso Ingegneri Associati (SRIA), Torino

R. Vesipa¹, L. Ridolfi¹, S. Fellini “Revealing the Topological Drivers of Hydraulic Transients in Water Distribution Networks”, 2025

M. Hanif Chaudhry “Applied Hydraulic Transients” (3rd Edition), 2014

Valerio Milano, “Acquedotti – Guida alla progettazione”, 1996

Lu Xing, Lina Sela, “TSNet Documentation - Release 0.2.0”, 2020

Klise, K. A., Hart, D., Moriarty, D., Bynum, M. L., Murray, R., Burkhardt, J., & Haxton, T “Water Network Tool for Resilience (WNTR) User Manual”, 2017

Vesipa R. Civil and industrial hydraulic systems – Lectures material, 2025.

<https://tsnet.readthedocs.io/en/latest/> (TSNet official website)

<https://www.istat.it/>, Istituto Nazionale di Statistica (ISTAT)

https://www.harper-haines.com/page_pageid_6275/ (Harper Haines website)